2003-12-05

Delineation of mass movement prone areas by Landsat 7 and digitial image processing

Shiloh Marie Howland
Brigham Young University - Provo

DELINEATION OF MASS MOVEMENT-PRONE AREAS BY LANDSAT 7 AND DIGITAL IMAGE PROCESSING

by

Shiloh M. James Howland

A thesis submitted to the faculty of

Brigham Young University

In partial fulfillment of the requirements for the degree of

Master of Science

Department of Geology

Brigham Young University

December 2003

BRIGHAM YOUNG UNIVERSITY

GRADUATE COMMITTEE APPROVAL

of a thesis submitted by

Shiloh M. James Howland

This thesis has been read by each member of the following graduate committee and by majority vote has been found to be satisfactory.

_____	_____
Date	Eric H. Christiansen, Chair
_____	_____
Date	Stephen T. Nelson
_____	_____
Date	Bart J. Kowallis

BRIGHAM YOUNG UNIVERSITY

As chair of the candidate's graduate committee, I have read the thesis of Shiloh M. James Howland in its final form and have found that (1) its format, citations, and bibliographical style are consistent and acceptable and fulfill university and department style requirements; (2) its illustrative materials including figures, tables, and charts are in place; and (3) the final manuscript is satisfactory to the graduate committee and is ready for submission to the university library.

_____ _____

Date Eric H. Christiansen
Chair, Graduate Committee

Accepted for the Department

_____

Bart J. Kowallis
Graduate Coordinator

Accepted for the College

_____

Earl M. Woolley
Dean, College of Physical and Mathematical Sciences

ABSTRACT

DELINEATION OF MASS MOVEMENT-PRONE AREAS BY LANDSAT 7 AND DIGITAL IMAGE PROCESSING

Shiloh M. James Howland

Department of Geology

Master of Science

The problem of whether Landsat 7 data could be used to delineate areas prone to mass movement, particularly debris flows and landslides, was examined using three techniques: change detection in NDVI (Normalized Difference Vegetation Index), change detection in band 5, and the tasseled cap transformation. These techniques were applied to areas that had recently experienced mass movement: Layton, Davis County and Alpine, Spanish Fork Canyon and Santaquin, Utah County. No distinctive spectral characteristics were found with any of these techniques with two possible explanations: 1. That despite improved spatial resolution in Landat 7 over its predecessors and improved digital image processing capabilities, the resolution is still too low to detect these characteristics or 2. That the aspects of a slope that make it prone to mass movement are undetectable at any resolution by remote sensing.

Change detection in NDVI examined if areas that remained unchanged (defined as $\leq 5\%$ change) between August 14, 1999 and October 17, 1999 correlated to areas that are prone to mass movement. There was no correlation.

Change detection in band 5 was examined between August 14, 1999 and October 17, 1999, October 17, 1999 and May 28, 2000 and August 14, 1999 and May 28, 2000. An interesting result is that the Shurtz Lake and Thistle landslides (Spanish Fork Canyon) showed changes of greater than 30% during August 14, 1999 – October 17, 1999 and October 17, 1999 – May 28, 2000. These changes were limited to these landslides and not seen in abundance in surrounding areas. A similar localization of 30% change was seen in the Cedar Bench landslide (Layton) for the same time periods. There were no other correlations.

The tasseled cap transformation shows areas of dominate greenness, soil brightness or wetness. None of these factors had distinctive patterns in the areas studied when compared to surrounding, mass movement-prone areas so no conclusions can be drawn about the utility of the tasseled cap transformation as it relates to areas of potential mass movement.

ACKNOWLEDGEMENTS

This work could not have gone forward without the help of many people. I'm grateful for the guidance of Dr. Christiansen, Dr. Nelson and Dr. Kowallis who willingly took me on as a student. Their editing has greatly improved this paper and their support made its completion possible. I am appreciative to Dr. Mabey for the images and initial idea and Dr. Harris for serving on the first committee. My training in remote sensing comes from Dr. Gluch and Dr. Jackson of the Geography Department.

I am grateful to my parents, Gary and Tari James and my brother Christiaan James, for encouraging my love of science. And last of all to my husband, Jared Howland for his constant support and encouragement. This project is theirs as much as it is mine.

TABLE OF CONTENTS

LISTS OF TABLES AND FIGURES

TABLES

FIGURES

INTRODUCTION TO THE PROBLEM

Landslides are traditionally mapped using large-scale aerial photos and ground surveys. The research presented here is based on the hypothesis that landslide and debris flow prone areas have distinctive spectral characteristics that can be delineated using digital image processing and Landsat 7 Enhanced Thematic Mapper (ETM+) scenes. If these unique spectral characteristics exist and can be seen at the resolution of Landsat 7, it could aid in delineating areas that are likely to experience mass movement in advance of actually visiting the location, thus saving time in travel and in field work.

Remote sensing has already found numerous applications in botany, forestry, geography, and even bedrock geologic mapping. Remote sensing data cannot be used or interpreted in a vacuum, but must be understood based on ground truth. Ground truth is the training acquired by doing field work used to understand what the images show and how a particular land cover looks in a scene. Remote sensing data are most effectively used when the area in the image is familiar to the interpreter.

Remote sensing is broadly, or *maximally*, defined as "the acquisition of data about an object without touching it" (Jensen, 2000). A more practical definition is what Jensen (2000) calls the *minimal definition*: "the noncontact recording of information from the ultraviolet, visible, infrared, and microwave regions of the electromagnetic spectrum by means of instruments such as cameras, scanners, lasers, linear arrays, and/or area arrays located on platforms such as aircraft or spacecraft, and the analysis of acquired information by means of visual and digital image processing." Many aspects of

geological investigation can be considered as remote sensing maximally but not minimally.

Remote Sensing Background

A Landsat 7 scene is more than just a photograph from space. It is composed of eight layers or bands of data that can be recombined and manipulated so that the scene becomes useful. The scene contains all the data. The resolution of the panchromatic band is 15 m per pixel as opposed to 30 m per pixel for the visible and middle infrared bands and contains four times as many pixels. A pixel is a two-dimensional picture element that is the smallest non-divisible element of a digital image (Jensen, 1996).

Each pixel in each band has a brightness value (BV). A brightness value is an assigned value along an 8-bit gray scale ranging from 0 (black) to 255 (white). This value quantifies the amount of electromagnetic energy reflected, within a specific spectral range for each band, back to the receiver. A color image can be construed by looking at three gray-scale layers at one time. Each layer is displayed in a specific plane of color – red, green or blue to create a color image (Figure 1).

Background of the Landsat program

The Landsat program began in 1972 following the successful application of satellites to study weather (Jensen, 2000). This program was designed to study land features from satellites in the same way that weather patterns are studied. Landsat 1 was launched with the intent to demonstrate the usefulness of remote sensing for land based applications (Sheffner, 1999). Landsat 1 through Landsat 3 used the Multispectral Scanner (MSS)

instrument. These early satellites used four bands covering the green, red and near infrared parts of the spectrum at 79 m per pixel and a thermal infrared band at 240 m per pixel. Landsats 4 and 5 used the Thematic Mapper (TM) instrument which kept the same bands as the first three instruments but expanded the spectrum with a blue band and two middle infrared bands. Spatial resolution was improved for all previous bands from 79 m per pixel to 30 m per pixel and the thermal infrared band improved from 240 m per pixel to 120 m per pixel (Jensen, 1996).

Landsat 7 ETM+ was originally intended to include bands with 10 m per pixel for the visible, near infrared and thermal infrared bands (bands 1-5 and 7), a 5 m panchromatic band and stereo capability for a total of eight bands. However, when Landsat 6 failed to achieve orbit in 1993, many of these features were dropped and Landsat 6 capabilities were used in Landsat 7 to make up for the loss (Jensen, 1996). Landsat 7 was launched in 1999 and uses the Enhanced Thematic Mapper (ETM+) instrument (Table 1). The two major improvements are the addition of a panchromatic (0.52-0.90 μm) band with 15 m per pixel spatial resolution and the improved resolution

TABLE 1. PROPERTIES OF LANDSAT 7 ETM+

Region of electromagnetic spectrum covered	Band Number	Spectral Range (μm)	Ground Resolution (m)
Blue	1	0.45 to 0.515	30
Green	2	0.525 to 0.605	30
Red	3	0.63 to 0.690	30
Near infrared	4	0.75 to 0.90	30
Middle infrared	5	1.55 to 1.75	30
Thermal infrared	6	10.40 to 12.5	60
Middle infrared	7	2.09 to 2.35	30
Green, red, near infrared	Pan-chromatic	0.52 to 0.90	15

of the thermal infrared band from 120 m on Landsat 5 to 60 m.

Summary of Images used in this Study

The Landsat 7 images used in this study were from Path 38, Row 32 (using the Path and Row Worldwide Referencing System) from August 14, 1999, October 17, 1999 and May 28, 2000 (Figure 2). Each scene is 185 km by 185 km.

Landsat 7 scenes are available from the EROS Data Center (http://edc.usgs.gov). All four scenes were radiometrically and geometrically rectified prior to distribution. All scenes use UTM coordinates and the WGS84 spheroid.

The landslide/debris flow events to occur after the imagery was sensed were the debris flows in Alpine and Santaquin/Spring Lake of September 2002. No known landslide events occurred within the area studied between August 1999 and May 2000.

Previous Work

The earliest published application of Landsat imagery to mass movement problems was by Sauchyn and Trench (1978). They used Landsat Multispectral Scanner (MSS) imagery to attempt to map landslides in Colorado. The authors hypothesized that because Landsat images are repetitive (every 18 days for the Landsats 1-3) and offered a wide variety of bands (four), that they may be able to delineate landslide features. Sauchyn and Trench (1978) identified that when mottling was present in the image, it could be a function of hummocky terrain. This hummocky terrain is assumed to be the result of previous mass movement. However, they were quick to point out that glacial

drift can have similar mottling. Scarps were observed to be most obvious in the near infrared band due to enhancement of shadows and possibly vegetation differences. They make several points which are still valid despite improved resolution and software capabilities. They assert that the limitations of Landsat images in identifying landslide prone areas is a result of landslides lacking unique spectral characteristics and that the scale of Landsat images is insufficiently fine to distinguish these areas. The lack of these unique spectral characteristics is due primarily to the fact that landslides can occur in an array of surificial materials. They conclude that landslide prone areas have no unique spectral appearance on Landsat images.

McKean et al (1991) evaluated remote sensing as applied to landslide hazard analysis in California and Oregon. They used remote sensing to map vegetation patterns and from this, infer debris flow susceptible landforms. In addition, they also performed a supervised classification of vegetation at several times, assuming that vegetation serves as a proxy for soil conditions. They found a correlation between greenness and soil depth with greenness defined by a Kahunen-Loeve transformation (Principle Components Analysis) of NS001 data. NS001 data is a simulation of Landsat 7 data which uses a multispectral scanner flown in a large aircraft to collect data from the ground in roughly the same range of the electromagnetic spectrum as Landsat 7. However, the resolution is much finer and the area to be studied can be targeted more directly. The scale and location of NS001 imagery is determined by the researcher who then specifies what altitude the aircraft should be flown. Greenness is measured by the amount of reflectance in the near infrared range but the specific definition of greenness can be adapted to individual problems. In another application, McKean et al. (1991) also used Airborne

Synthetic Aperture Radar (at approximately 30 m per pixel spatial resolution) to study a forested earthflow in Oregon that showed an increase in brightness in band 4 (near infrared) as flow speed increased. As the earthflow moved faster, it toppled pine trees, exposing the deciduous undergrowth which explains why band 4 brightened with increased flow speed. Near infrared, middle infrared/near infrared and greenness indices were all able to detect major colluvial deposits that correlate with actual soil depths.

An interesting approach using Landsat 4 images, the Normalized Difference Vegetation Index (NDVI) and landslide mapping came from Samarakoon et al. (1993). By comparing scenes from September and November for the Yoshino river basin in Japan, they discovered areas that remained high in greenness (high NDVI) in both the wet (September) and dry (November) seasons. It was inferred that these areas had higher soil moisture and could be more susceptible to mass movements. The NDVI was a proxy for the "state" or amount of groundwater and it can partly compensate for illumination conditions and atmospheric effects. The resultant image of high moisture areas was then compared to previously mapped landslides. Upon comparison, it was found that most of the estimated high-moisture areas as determined by interpretation of the satellite images were distributed over landslide prone areas.

A technique using both Landsat 4 Thematic Mapper (TM) data and Synthetic Aperture Radar (SAR) was used to locate retrogressive slope failures in shale along the Saskatchewan River by Shih and Jordan (1993). They comment that the spatial resolution of Landsat 4 TM and SPOT (Systeme pour l'Observation de la Terre) data is generally not fine enough for landslide characterization. For this purpose, they re-sampled the TM data with the SAR data to achieve a smaller effective spatial resolution.

Landslides in the Saskatchewan Valley were easily seen on SAR and re-sampled SAR/TM scenes because of their large size, poorly vegetated surfaces, and morphologies. Landslides were generally found near areas of active river erosion. Shih and Jordan (1993) concluded that their methodology is useful in characterizing landslides in both high and low relief areas. They make no comment on spectral characteristics of areas that may experience landslides, only that landslides can be seen on SAR and re-sampled SAR/TM scenes.

Objective

The objective of this study was to determine if the improvements in the resolution of Landsat 7 ETM+ and the availability of more advanced digital imaging software could be used to identify mass movement prone areas. This was to be accomplished by building upon previous work and specifically by using several Landsat 7 ETM+ images and ERDAS Imagine 8.5 software to study the landslides and debris flows of the Wasatch Front, central Utah.

Summary and History of Wasatch Front Mass Movement Events

Specifically, this research focuses on four areas of mass movement activity along the Wasatch Front and 11 specific landslides or debris flows within those areas. Selection of these areas guided by Dr. Matthew Mabey of Brigham Young University and to overlap research being done by Francis Ashland of the Utah Geological Survey. The four areas, from north to south, are listed below; the number in brackets indicates years of notable or measurable movement:

1. Layton
    A. Heather Drive landslide [2001]
    B. Sunset Drive landslide [1998]
    C. South Fork Kays Creek landslide [1984, 1998]
    D. Cedar Bench landslide [1998]
    E. South Weber Drive landslide [1983, 1984, 1998]
2. Alpine
    A. Preston Canyon debris flows [2002]
3. Spanish Fork Canyon
    A. Thistle Slide [1983, 1998]
    B. Shurtz Lake landslide [1997]
    C. Joes Canyon debris flow [1998]
4. Santaquin
    A. Two un-named debris flows from Dry Mountain tributaries 4 and 5 [2002]

Because the images are fairly recent, ranging from August 1999 to May 2000, landslides/debris flows were selected that had occurred between 1997 and 2002. For this study to be valid, it was assumed that conditions at the time of imaging were comparable to real ground conditions in 1997 to 2002. This may not be a valid assumption as 1998 was the fifth wettest year on record for Utah and subsequent years have been much drier. Also, landslides/debris flows had to be selected for study that were within the Landsat 7 scenes.

This research examines landslide areas after the fact with the hypothesis that some feature(s) would be unique. If found, these features could be applied to other mass movement prone areas and aid in prediction of future events of mass movement. Specifically, comparable areas located near landslides were studied; comparable being defined as similar geomorphology, slope, vegetation, and surficial geology. For example, in Spanish Fork Canyon, the hummocky terrain between the Shurtz Lake and Thistle slides is assumed to be a potential source for future mass movement events. This assumption is made because the terrain is interpreted as previous mass movement events

and it seems likely that because of the steep slope and history of mass movement events, this area will move again. Likewise, the drainage of Joes Canyon, also in Spanish Fork Canyon, is compared to nearby Sterling Hollow. Therefore, it was not the actual landslide or debris flow being studied but the areas in the vicinity of the slide or flow that seems most likely to have an event in the future.

Layton

Layton City has experienced five major landslides in the last five years, notably along the valley walls of Kays Creek and primarily as a result of the 1998 wet year. Five landslides in Layton are used in this study (Figures 3, 4, and 5). The Layton landslides all occurred within transgessive Lake Bonneville deposits of latest Pleistocene age (Giraud, 1998a). Subsequently, rivers have cut down through these silty to gravelly deposits creating steep, unstable valley walls. The valley walls of Kays Creek were mapped as landslide deposits as early as 1975 (Kaliser and Slosson, 1988) and all the recent (1998-2001) landslides occurred in areas of previous movement.

Heather Drive. The Heather Drive landslide in Layton moved as early as August 1998 when homeowners had to repair driveways and noticed foundation cracks (Figure 6). Movement continued at a slow rate until late August 2001 when it failed rapidly (Giraud, 2002b). This landslide is unusual because it continued in late summer during a year with below-average precipitation. The Heather Drive landslide was the only Layton landslide to occur in 2001. The scarp (410 m long and 3 m high) follows an arcuate crest which was interpreted as a reactivation of a previous landslide (Giraud, 2002b).

Sunset Drive. The Sunset Drive landslide occurred near 1851 East Sunset Drive (lot 105) in Layton in April 1998 (Giraud, 1998a). It occurred on the same northwest facing valley wall of South Fork Kays Creek as the South Fork Kays Creek and Heather Drive landslides. Houses in the area experienced exterior damage including displaced foundations, tilted and bowed walls and damaged door frames. Houses on the surrounding lots suffered ground cracks in foundations, displaced driveway slabs and gaps in between the driveway, garage and elsewhere (Giraud, 1998a). The crest of surrounding lots 104-108 is scallop-shaped which is interpreted by Giraud as being formed by previous landslide movement. A stream has incised the Weber River Bonneville delta and exposed lacustrine sediments that are prone to landsliding (Giraud, 1998a). The only visible geomorphic features are two scarps (maximum height of 30 cm) that may not be related to each other and 1.3 cm wide ground cracks. Giraud notes in his report that this area is susceptible to future landslide events.

South Fork Kays Creek. A landslide along South Fork Kays Creek (Giraud, 1998b) occurred in April 1998 in the vicinity of 1050 East and 1530 North in the city of Layton. Movement displaced turf, curbs, chain link fences and a rock wall. This event occurred in on the same north-facing bluff as the Sunset Drive and Heather Drive landslides, which has been mapped as prehistoric landslide deposit. The 1984 landslide scarp on this bluff is visible on 1985 aerial photos but has since been re-graded and filled (Giraud, 1998b). The scarp of the 1998 landslide has a similar length, shape and position to the 1984 scarp. At its maximum, the 1998 scarp was 1 m high. As the stream continues to erode the toe of the 1998 slide, movement will likely continue (Giraud, 1998b).

Cedar Bench. The April 1998 Cedar Bench landslide occurred on the same northeast-facing bluff as the 1984 and 1998 South Weber landslides. The landslide occurred just above the Cedar Bench subdivision on a bluff with an average gradient of 35% (Solomon, 1998). The 1998 landslide was a composite slide that possibly reactivated older, deep-seated earth slides and flows. The area is a complex of shallow slides about 120 m wide with a maximum scarp height of 2.5 m (Christenson, 1998). In 1998, precipitation for January through April was 147% of average and the landsliding is believed to be a result of increased pore pressure (Christenson, 1998).

South Weber Drive. The 1998 landslide occurred on the eastern edge of South Weber landslide complex which is a zone of prehistorical and historical landsliding (Figure 7). The entire slope moved in spring 1984. The 1998 slide occurred in a zone of slumps and slides about 75 m long and 360 m wide. The scarp was up to 1.8 m high and all movement appeared to be shallow and did not affect the Davis-Weber canal (Black, 1998). Black noted that landsliding began due to marginal slope stability and elevated groundwater levels, but the exact cause for movement is still unclear. Precipitation in the area in January and February of 1998 was 200% of normal precipitation (Giraud, 1998).

This same area (south of South Weber Drive) had a rotational slide activated in 1983. It reactivated along the lines of an ancient slide mass and at least one small debris flow occurred historically at the toe of the landslide (Kaliser and Slosson, 1988). Maps of the South Weber Drive area show landslide events in 1984 and 1998 (Lund, 1984; Black, 1998).

Alpine

The City of Alpine in northern Utah County experienced two debris flows in an eight day period in September, 2002, both emanating from Preston Canyon (Figures 8, 9, and 10). No previous landslide or mass movement maps show debris flows emanating from this canyon. In nearby American Fork Canyon, 27 landslide/debris flow events occurred in 1983 (Brabb, Wieczorek, and Harp, 1989).

Preston and Willow canyons are narrow canyons incised into the Precambrian Mineral Fork Tillite and the Cambrian Mutual Formation (quartzite) and Tintic Quartzite (Baker and Crittenden, 1961). The head of each canyon is composed of Mississippian age limestones. There are Pleistocene – Holocene age debris flow deposits at the mouths of each canyon (Machette, 1992)

Preston Canyon. The City of Alpine was affected by two debris flows on September 8 and 16, 2002. By September 8, 2002, Alpine had received 3.9 cm of rain in 48 hours (Warnock, 2002). This debris flow damaged a home at 87 N Bald Mountain Drive. Richard Giraud of the Utah Geological Survey visited Alpine between the two debris flow events and mapped the September 8 flow.

On September 16, 2002, Alpine received 1.4 cm of rain in 24 hours which initiated the first debris flow. This flow began in a north facing tributary of Preston Canyon. This second flow was examined by the author on September 18, 2002. At Preston Canyon Drive, it was about 45 m wide (Figure 11). Farther east, the channel was 2 m deep (Figure 12). Boulders up to 45 cm across had been entrained and lighter, organic float such as dead branches were entrained perpendicular to the direction of flow. The September 8 flow broke through to Bald Mountain Drive on an undeveloped lot,

which shows evidence of previous debris flow events but no events have been mapped in this area.

Spanish Fork Canyon

Spanish Fork Canyon is a mass movement-prone area, known primarily for the Thistle slide in 1983. It has also experienced more recent movement in Thistle slide itself and surrounding areas (Figures 13, 14 and 15).

Joes Canyon and Sterling Hollow are canyons that incise two sandstone units – the Permian Diamond Creek sandstone and the Oquirrh Formation (Witkind and Page, 1983). At the mouths of each canyon are lacustrine gravel deposits from Lake Bonneville and fan alluvium that predates Lake Bonneville (Machette, 1992). The Shurtz Lake and Thistle landslides both emanated from the Tertiary North Horn Formation which consists of mudstone, sandstone, limestone and conglomerate layers. The mudstone is unstable when wet and has a tendency to slump (Witkind and Page, 1983). There are also older landslide deposits in the area of Thistle slide (Witkind and Page, 1983).

The most remarkable historic movement of Thistle slide followed seven months of above-normal precipitation in April 1983. Within a week, the landslide dammed the river and formed 'Thistle Lake'. Thistle Lake reached its peak on June 2, 1983 with a volume of 8000 hectare-meters and depth of 55 m. (Slosson et al.., 1992; Slosson & Kaliser, 1988; Ashland, 2002). Thistle Slide was active prior to 1983 and had been mapped as early as 1955 and described by Rigby and Hintze in 1962 (Schroder, 1971).

Thistle. The Thistle landslide reactivated most recently in May, 1998 (Figure 16). Movement was initiated by the detachment of a large slump block at the crown of the landslide. The detachment and rotation of the slump block created a vertical scarp of nearly 30 m in height. Most movement occurred by sliding on the deep 1983 rupture. Relative displacement of casings oriented east-west suggests a minimum of approximately 48 m of movement (this value may include 1997 movement) (Christenson, 1998). Average rates of movement for years prior to 1997-8 were about 0.17 m/yr yielding about 2.4 m of movement that would have occurred from 1984-1998 (Christenson, 1998). The entire landslide, except for the dam, moved in 1998 (Christenson, 1998). The spring of 1998 was the third wettest on record for Spanish Fork Canyon and surpassed only by 1982 and 1983 (Figure 17) (Ashland, 2003).

The southeast side of Thistle landslide had partially reactivated in 1997, the fifth wettest year on record. Folds and scarps were visible as early as March, 1997 and confirmed in September.

Shurtz Lake. The Shurtz Lake landslide occurred in early May 1997 displacing Utah Power and Light high voltage power lines. The landslide is a composite body with two earth flows that are visible from State Highway 6 (Figure 18). With the snowmelt in March 1998, the slide reactivated and achieved a maximum displacement of 20 m along its left flank. Both episodes of movement were preceded by above-normal precipitation.

Shurtz Lake slide is only 1.5 km north of Thistle slide and shares some geologic similarities with Thistle in that both emanated from the North Horn Formation. There is no evidence of the Shurtz Lake area moving since at least 1923 when the power lines were installed on the slope (Ashland, 2003). The Shurtz Lake slide occurred in

prehistoric hummocky landslide deposits that are visible in large-scale aerial photos from 1983 (Ashland, 2003). Ashland (2003) asserts that the Shurtz Lake slide is only dormant and not yet stabilized.

Joes Canyon. The third event in Spanish Fork Canyon in 1998 was a debris flow in late April in Joes Canyon, a deep narrow channel. Superelevation extended to 20 m above the channel of 3 m flow depth, as estimated by vegetation disturbances (Ashland, 2003) (Figure 19). At the mouth of Joes Canyon, the debris flow created a levee (Figure 20) and fan (Figure 21) of lighter organic materials. Evidence of previous movement in this canyon is found on aerial photographs from 1984 showing a debris flow that occurred previously, most likely just a few years before (Ashland, 2003).

Santaquin

Santaquin and Spring Lake experienced five major debris flows on September 12, 2002, within the same week of the Alpine debris flows. Two flows, emanating from tributaries 4 and 5, are examined in detail (Figures 22 and 23). The flows have no official name but based on the Utah Geological Survey report and the burned-area emergency rehabilitation (BAER) report, they will be called the Tributary 4 and Tributary 5 debris flows for this report (McDonald and Giraud, 2002 and U.S. Forest Service, 2001).

The Tributary 4 and 5 flows emanated from two large canyons on the northern end of the west slope of Dry Mountain. The other large flows came from Tributaries 6, 3 and 2 and the small flows came from Tributaries 7, 9, 11, 12, and 14 (McDonald and Giraud, 2002). Dry Mountain consists of a succession of rock units ranging from the

mid-Proterozoic to the Mississippian. These units include the Archean/Proterozoic Santaquin Canyon complex, Proterozoic Big Cottonwood Formation, Cambrian Tintic Quartzite and Ophir Shale and Mississippian Gardison and Deseret limestones (Witkind and Wise, 1991).

Events leading up to the Santaquin debris flows began a year prior with the Mollie Fire, which burned the Dry Mountain drainages in their entirety between August 18 and September 1, 2001 with the mostly intensely burnt areas on the north-facing slopes of the tributaries of Dry Mountain (Hardy, 2001 and U.S. Forest Service, 2001) (Figure 24). An article in the Deseret News from October 16, 2001 warned residents to consider flood insurance (Hardy, 2001). The same article stated that there was no vegetation above the subdivisions on the east side and it would only take 0.60 cm to 1.30 cm of rain in a half-hour to cause debris flows (Hardy, 2001) and on September 12, 2002, Santaquin received 1.4 cm of rain (McDonald and Giraud, 2002). Although the slopes were seeded after the fire, the continuing drought made it difficult for the seeds to gain a foothold (Hardy, 2002b). It is noted in the BAER report that there was a heightened debris-flow risk following the Mollie fire (U.S. Forest Service, 2001).

The United States Forest Service installed jersey barriers at 900 East from 150 to 450 South in an attempt to protect structures. The 2002 debris flows hit about a half mile north of the barriers at 300 North (City of Santaquin, 2003). Previous mass movement in this area includes a landslide mapped near Spring Lake during the 1983 wet year (Brabb at al., 1989).

Tributary 4 and 5 debris flows. On September 12, 2002, two large debris flows traveled west from Dry Mountain and damaged homes in Spring Lake and Santaquin,

Utah County (Figure 25). The hazard for debris flows on Dry Mountain existed prior to the fire and will exist even once the vegetation recovers (McDonald and Giraud, 2002).

ERDAS IMAGINE 8.5 AND IMAGE PROCESSING TECHNIQUES

To determine if debris flow/landslide prone areas have distinctive spectral characteristics, three image processing techniques were used with ERDAS Imagine 8.5. ERDAS Imagine 8.5 is a powerful digital image processing program that permits the analyst to perform a wide array of image processing techniques very quickly. The three techniques examined in this research are:

1. Change detection using the Normalized Difference Vegetation Index
2. Change detection of band 5
3. Tasseled cap transformation

The spectral characteristics of debris flow and landslide prone areas are not well known. However, change detection using the Normalized Difference Vegetation Index and a precursor to the technique using band 5 have shown some potential. The remaining technique, tasseled cap transformation, was used because it employs parameters important to mass movement.

No technique, or combination of techniques, was successful in delineating distinctive characteristics of landslide/debris flow prone areas in the Wasatch Mountains. For a small region such as the slopes of South Fork Kays Creek in Layton, it was expected that the recently active slopes would have a signature that was specific to the active area and that inactive areas would not have that same signature. For a larger region, such as Spanish Fork Canyon, it was hypothesized that some part(s) within the landslide/debris flow prone areas would have a distinct signature on a Landsat 7 image that could be related to unique conditions on the ground. Ideally, these ground conditions

would be favorable for initiating mass movement. It seems clear now that there are two explanations for the lack of distinctive features: that the imagery spatial resolution is still too low in resolution to discern those differences or there are no surface differences and initiation of mass movement is based on other factors such as weather or subsurface conditions that cannot be measured by Landsat 7.

CHANGE DETECTION OF THE NORMALIZED DIFFERENCE VEGETATION INDEX (NDVI)

The Normalized Difference Vegetation Index (NDVI) is a measure of greenness assessed using the formula NDVI = ($BV_{\text{near infrared}}$ - BV_{red}) / ($BV_{\text{near infrared}}$ + BV_{red}) for each pixel of the scene. Specifically for Landsat 7, the formula is NDVI = ($BV_{\text{Band 4}}$ – $BV_{\text{Band 3}}$) / ($BV_{\text{Band 4}}$ + $BV_{\text{Band 3}}$) where *BV* is the brightness value for each pixel in each band. Change detection is a simple mathematical subtraction of the later NDVI image from the earlier NDVI image.

Samarakoon et al. (1993) used change detection with NDVI images from different times (September and November) to find areas that had high NDVI and that remained unchanged during the intervening time correlated to previously mapped landslides. This technique was used to answer the question: do areas that remained unchanged over a period of time correlate to landslide/debris flow prone areas? If an area remains unchanged in greenness/NDVI for a significant period of time, it is hypothesized that this is due to unchanged groundwater conditions that could be favorable for mass movement. Samarakoon et al.'s (1993) work studied the Yoshino river basin in Japan, which receives an average of 2.5 m of rain every year, a value which is in marked contrast to the limited amount of rain (0.6 cm annually) that the Wasatch Mountains of Utah receive. (National Weather Service, 2003)

An NDVI image is a gray-scale image that shows bright areas of high NDVI and dark areas of low NDVI. If this technique had been successful at correlating unchanged

areas to mass movement prone areas, places of high NDVI that remained unchanged would have been seen from the August 1999 scene to the October 1999 scene. These two dates were used because they most closely correspond to the August-November comparison that Samarakoon et al., used. To increase the chance that it would detect areas where change would be close to zero, the change detection algorithm limits were set at ± 5%. A change in percentage instead of a change in number of brightness values is used to narrow the range of change that would show "no change." The use of percentages in change means that the brighter NDVI areas in particular have less freedom to change before they leave the bounds set as equaling 'no change.'

Although the results show that some actual landslides change differently when compared to surrounding areas, the results do not support the general hypothesis that landslide/debris flow prone areas have distinctive spectral characteristics relative to NDVI. Areas of positive NDVI change show as bright green and negative change appears as bright red. The change detection layer in each subset is displayed over a band 8 scene from May 28, 2000 of the area.

Layton

Change in NDVI in the Layton subset for August 14, 1999 and October 17, 1999 shows a predominant ≥ 5% decrease in the study areas (Figure 26). The bluffs of all five landslides, including the areas of the recently active landslide all show this decrease. The bluffs themselves are well delineated as areas of ≥ 5% decrease with one small exception – the area just north of the Heather Drive landslide. This area is a gently undulating, but not hummocky, grassy slope and not as steep as the bluffs on which all the landslides occurred. For this reason, there is hesitation to draw the conclusion that the lack of

change between August and October alone suggests that conditions are favorable for mass movement. This is a good example of why remote sensing cannot be examined without ground truth or this area may have been mistakenly categorized as primed for movement. Most areas that show no change are not vegetated to begin with, so should not have any change in NDVI.

Alpine

Change detection analysis for the Alpine subset between August 18, 1999 and October 17, 1999 show most of the mountainous areas as having a ≥ 5% decrease between these two dates (Figure 27). Again, this would be expected during fall as plants begin to die. The distribution of unchanged areas in Preston and Willow canyons is similar so no conclusions can be drawn from this data that might explain why Preston Canyon experienced debris flows in September 2002 and Willow Canyon did not.

Spanish Fork Canyon

Change detection analysis for the Spanish Fork Canyon area between August 14, 1999 and October 17, 1999 shows nearly the entire scene as having a ≥ 5% decrease between these two dates (Figure 28). This is predictable in that much vegetation begins to die by mid-October so a reduction in NDVI is expected. Notably, parts of Thistle slide and Shurtz Lake landslide remain unchanged as do some of the un-vegetated slopes at the bottom of the area. Although this analysis does not offer any indications of potential movement in the study area between Thistle and Shurtz Lake landslides, the lack of change on the landslides themselves could mean that those areas are still active. In the Sterling Hollow study area, there are no unchanged areas so no conclusions can be drawn

about the potential for mass movement in that canyon from this analysis. The large green area (≥ 5% increase) on the east side of the image is a cloud on the August 14, 1999 image.

Santaquin

Change detection between August 14, 1999 and October 17, 1999 of the Santaquin subset shows that the Dry Mountain study area, including Tributaries 4 and 5, uniformly shows a ≥ 5% decrease (Figure 29). The distribution of unchanged areas is consistent between Tributaries 4 and 5 which experienced debris flows in September, 2002 and the other canyons that did not. Therefore, no conclusions can be drawn about why Tributaries 4 and 5 experienced debris flows but other nearby canyons to the south did not.

Conclusions

The climate difference is the most probable explanation for why this technique was not particularly useful in delineating any distinctive NDVI features that correlate to areas of mass movement. Another explanation could be that the factors that caused mass movement cannot be identified with this technique, regardless of climate.

CHANGE DETECTION IN BAND 5

Band 5 (1.55-1.75 μm) is one of the two middle infrared (MIR) bands, the other being band 7 (2.08 – 2.35 μm). Band 5 is sensitive to the amount of water in plants and soil and can be used in crop drought investigation and in measuring plant vigor (Jensen, 1996). The theoretical basis for this work was to see how soil moisture changed over time in landslide/debris flow-prone areas and if any assumed landslide/debris flow-prone areas had significant difference from other areas. A low brightness value in band 5 means an area is wet or moist.

Shallow landslides may be a result of increased soil moisture. For this reason, change detection was used to determine how soil moisture (band 5) responded through time. This met with some interesting results in Spanish Fork Canyon, so the technique was attempted at the other locations. For this reason, Spanish Fork Canyon is discussed first in this section.

Change detection was examined between August 14, 1999 and October17, 1999, October 17, 1999 and May 28, 2000, and August 14, 1999 and May 28, 2000 to see how the brightness values changed. The technique was used with values of ± 10% and ± 30%. After experimenting using the Spanish Fork Canyon subset, it was determined that these values were the most useful because they highlighted the differences between Thistle and Shurtz Lake landslides compared to the surrounding areas. Spanish Fork Canyon was used as the training ground for this technique because it is such a large area of potential landslides. Change detection highlights pixels that changed ≥ 10% or ≥ 30% between the

two dates. Percentages were used instead of brightness values to focus on significant fluctuations.

Some work has been done previously using band 6. A study by Shih and Jordan (1993) found a correlation between the response of Landsat 5's thermal infrared band 6 and qualitative soil moisture. Landsat 7 has a TIR band with resolution of 60 m; a great improvement over the 120 m resolution of Landsat 5 which will allow better resolution of areas of differing soil moisture. Despite having the lowest resolution of the eight bands at 60 m, band 6 may offer the most data as it responds to soil moisture and temperature (Mantovani et al., 1996). Change detection was attempted with band 6 in the Spanish Fork Canyon subset and there were no distinctive results for any of the landslide prone areas. In band 6, there is an insignificant difference, usually less than 30 brightness values, between the lowest value and the highest value of a scene, whereas band 5 generally has a difference of 150 brightness values. This significant range of brightness values along with its relationship to soil moisture, making examination of band 5 valuable.

Spanish Fork Canyon

This analysis focused on the study area between Shurtz Lake and Thistle slides and Sterling Hollow. If this technique were successful, these study areas would change differently compared to other nearby areas.

At ± 10% for the change between August 14, 1999-October 17, 1999, the area between Thistle and Shurtz Lake slides show a ≥ 10% decrease in brightness value for this time period and predominately in less vegetated areas (Figure 30). Thistle slide is well delineated by the otherwise sporadic patches of ≥ 10% decrease. The Shurtz Lake

slide is not as well delineated but the concentration of areas with ≥ 10% decrease are more dense near the slide. Joes Canyon and Sterling Hollow have similar areas of decrease and increase. Joes Canyon does not look different from Sterling so no conclusions can be drawn from this data. The large red area on the eastern edge of the image is a cloud. This cloud appears as an anomaly on the October 17, 1999 scene.

At ±30%, Thistle slide and Shurtz Lake slide have a higher concentration of areas of ≥ 30% decrease than the study area between the two landslides, which means some unique soil moisture conditions may exist within the landslides themselves (Figure 31). Joes Canyon and Sterling Hollow have a few minor drainages with ≥ 30% decrease but because they both do, it is not significant.

At ±10% for the time between October 17, 1999 and May 28, 2000, Thistle and Shurtz Lake slides show an increase of ≥ 10%, the expected and reverse change seen between August 14, 1999 and May 28, 2000 (Figure 32). Sterling and Joes Canyons have similar characteristics – the sunlit side showing a ≥ 10% decrease and the shadowed (west facing) side showing a ≥ 10 increase in brightness values for Band 5. At 30% for this same time frame, Thistle and Shurtz Lake slides show an increase of ≥ 30% and a fairly high concentration of pixels showing a change (Figure 33). The areas between the two slides have a few, very small areas of change. Sterling and Joes Canyons again have a few minor drainages showing a ≥ 30% increase but because the areas of increase are similar in size and respective location, it is insignificant.

Between August 14, 1999 and May 28, 2000, the ± 10% change shows that Thistle and Shurtz Lake slides themselves show a ≥ 10% decrease for the time period (Figure 33). This is significant in that the surrounding areas show a ≥ 10% increase for

the same time. This shows that the landslides themselves have some distinctive soil moisture properties that are not seen in nearby areas. There are no significant observations of Joes Canyon and Sterling Hollow for these dates. At ± 30%, a few small areas within Thistle and Shurtz Lake landslides themselves show a ≥ 30% decrease (Figure 34). Most of the study area shows no change at this value so the ≥ 30% decrease in the landslides again shows some significant differences between the landslides and the surrounding area.

The results in Spanish Fork Canyon were interesting and it was anticipated that other areas would show similar responses when comparing band 5 over the available time frame. However, even the few results seen in Spanish Fork Canyon were not replicable in other areas. Although the images are included, there is nothing truly interesting about the results. This study can conclude tentatively that the soil moisture conditions present in landslides, but not landslide-prone areas, are distinct even years after they have moved but cannot actually say what those conditions are unless the area was studied with more recent images. Unfortunately for this study, the study areas that are considered prone to future debris flows/landslides lack any unique soil moisture characteristics that could be identified by change detection in band 5.

Layton

The Layton area is more complex because of the numerous landslides within a residential area. This study only focuses on the five landslides as discussed in the Background section of this paper. Also, the bluffs that have been actively moving – North and South Forks of Kays Creek and the bluff on the south side of the Davis-Weber Canal – are considered to be the best locations for future landslides. For this technique to

be successful, the areas that have moved recently should have results that differ from nearby areas.

For the time between August 14, 1999 and October 17, 1999, change detection for ±10% shows an area of ≥ 10% decrease in the vicinity of South Weber Drive and Cedar Bench landslides (Figure 36). The slope of South Fork and North Forks of Kays Creek show a ≥ 10% decrease but the lowest part of the slope shows no change at 10%. For ±30% in the same time frame, the slopes remain unchanged with scattered areas of ≥ 30% decrease (Figure 37). Recently active landslide areas appear no different from inactive but potential landslide areas.

As with Spanish Fork Canyon and the other areas in this study, the areas of increase or decrease reverse when looking at the October 17, 1999-May 28, 2000 timeframe. However, at ±10%, there is a ≥ 10% increase in area of South Weber Drive/Cedar Bench landslides and the slopes of South Fork Kays Creek (Figure 38). Some areas in the deepest part of the drainages remain unchanged for this time period. This seems unusual that the increased moisture of spring would not affect the soil moisture conditions. Unfortunately, unchanged areas do not correlate to any recently active landslides and because they are in the bottom of the drainage, it is unlikely that they will move. At ±30%, the area of the Cedar Bench landslide shows a ≥ 30% increase (Figure 39). Except for a few very small, scattered areas of ≥ 30% increase, this is the only location with any interesting results. The location of a retention pond in the vicinity of the landslide may skew the result.

The August 14, 1999 and May 28, 2000 scenes are so close that change detection between those two scenes may be the only valid way of studying this problem. For the

changes between August 14, 1999 – May 28, 2000 at ±10%, the grassy area north of the Heather Drive landslide and the slope coincident with the Cedar Bench landslide have a marked decrease at ±10% (Figure 40) but minimal at ±30% (Figure 41). The rest of the bluff for the South Fork Kays Creek area, Cedar Bench, and Sunset Drive and South Weber landslides showed no changes ≥ 30% between August 14, 1999 and May 28, 2000.

Alpine

As with all other techniques, the analysis of changes in band 5 is examined in two canyons: Preston Canyon and Willow Canyon. It assumed that except for Preston Canyon experiencing a debris flow, both canyons share similar characteristics as far as soil moisture, slope, and other variables are concerned. If the hypothesis was correct, it would be expected that Preston Canyon would have a different response in band 5 than Willow Canyon over time. Ideally, this different reaction would be unique to Preston Canyon and evidence of its future movement potential. It can be argued that conditions have changed over time but for this study, only these images were available.

Band 5 is compared between August 14, 1999 and October 17, 1999. At ±10% change, Preston and Willow Canyons look similar (Figure 42). The south-facing slopes have areas of ≥ 10% change but most of the slopes showed a ≥ 10% change, including the drainage on the north-facing slope from which the September 2002 debris flows originated. At ±30%, Preston Canyon has a few small areas in the canyon bottom and on the north-facing slope that shows a ≥ 30% decrease (Figure 43). Willow Canyon lacks any changes at ±30%. If the areas of ≥ 30% decrease occurred in the drainage that

initiated the debris flow, there may be some correlation. As this is not the case, nothing can be concluded from this analysis.

Comparing band 5 between October 17, 1999 and May 28, 2000 shows the expected results. Most of the mountain slope shows a ≥ 10% increase in brightness between these two dates (Figure 44). This area includes the drainage of the September 2002 debris flow events. At ±30%, a few small areas in the floor of Preston Canyon and on the north-facing slope of Willow Canyon show a ≥ 30% increase (Figure 45). None of those areas coincide with the drainage causing the September 2002 event.

Between August 14, 1999 and May 28, 2000, at ± 10% most of the slope shows a ≥ 10% increase in that time (Figure 46). A notable exception is the bowl in the upper part of Preston Canyon where the September 2002 debris originated. There are no changes at ±30% (Figure 47). This is interesting but it is difficult to draw conclusions from this because the drainage of most interest is in the shadows in both scenes. At best, this result is inconclusive because it is difficult to draw any conclusions from the shadowed data.

Santaquin

For the Dry Mountain debris flows, the changes seen in Tributaries 4 and 5 were compared with other canyons on the same slope. It is assumed that all were burned equally in the August/September 2001 fires (confirmed by the initial BAER report), have the same slope and same basic conditions. The debris flows for both canyons initiated in the various feeder drainages at the upper bowls of the canyons.

Between August 14, 1999 and October 17, 1999 at ± 10%, a ≥ 10% decrease is widespread over all of Dry Mountain (Figure 48). Most canyons, including Tributaries 4

and 5, have small areas of ≥ 10% increase on the sunlit, south facing slopes. Tributaries 4 and 5 have no characteristics that are unique to them. At ± 30% change, there are no changes (increase or decrease) for the Dry Mountain area (Figure 49).

Between October 17, 1999 and May 28, 2000 at 10%, a widespread ≥10% increase is seen on shadowed side of all canyons, including the upper reaches of Tributaries 4 and 5 where the debris flows initiated (Figure 50). At ±30%, Tributaries 4 and 5 show somewhat more areas of ≥ 30% increase compared to other canyons but these areas do not match the locations of the upper reaches of the canyons where the debris flows initiated (Figure 51).

At ± 10% for the time between August 14, 1999 and May 28, 2000, Tributaries 4 and 5 equally green (≥ 10% increase) compared to other canyons (Figure 52). An interesting note is that both north and south facing slopes of the canyons show a ≥ 10% increase. At ± 30% change, none of the slopes of the west side of Dry Mountain show any changes in either direction (Figure 53).

Essentially, there were no unique changes in the soil moisture of Tributaries 4 and 5 as compared to other canyons on Dry Mountain for any time period for which there is data.

Conclusions

This technique failed to delineate distinctive characteristics discernable by comparing band 5 across time. The interesting results are that the Shurtz Lake and Thistle landslides did show decreases and increases of ± 30% when surrounding areas did not.

TASSELED CAP TRANSFORMATION

The tasseled cap transformation or Kauth-Thomas transformation creates three new axes out of the original 6 axes (bands) of data for a Landsat 7 scene (the term 'tasseled cap' refers to the shape of the plot when brightness values for brightness are plotted against brightness values for greenness, see Figure 54) (Kauth and Thomas, 1976). The three new axes correspond with three indices: the soil brightness index, the

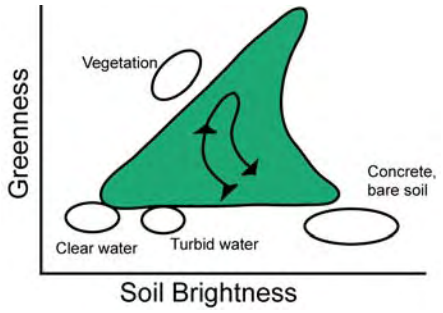

Figure 54: Conceptualization of the tasseled cap transformation. The path represents the path a pixel travels during the growing season

green vegetation index, and the wetness index (Jensen, 2000). For example, in the wetness index, wet areas have lower brightness values than drier areas. Brightness is a weighted sum of all bands and defined in the direction of the principal variation in soil reflectance. Greenness is orthogonal to brightness and a contrast between the near-infrared and visible bands. As expected, it is intended to correlate to the amount of green vegetation in a scene.

These three bands are shown with brightness in the red plane, greenness in the green plane and wetness in the blue plane. The algorithm for a tasseled cap transformation for Landsat 7 data is:

$$\text{Brightness} = 0.3037(BV_{\text{Band1}}) + 0.2793(BV_{\text{Band2}}) + 0.4743(BV_{\text{Band3}}) + 0.5585(BV_{\text{Band4}}) + 0.5082(BV_{\text{Band5}}) + 0.1863(BV_{\text{Band7}})$$

$$\text{Greenness} = -0.2848(BV_{\text{Band1}}) - 0.2435(BV_{\text{Band2}}) - 0.5436(BV_{\text{Band3}}) + 0.7243(BV_{\text{Band4}}) + 0.0840(BV_{\text{Band5}}) - 0.1800(BV_{\text{Band7}})$$

$$\text{Wetness} = 0.1509(BV_{\text{Band1}}) + 0.1973(BV_{\text{Band2}}) + 0.3179(BV_{\text{Band3}}) + 0.3406(BV_{\text{Band4}}) - 0.7112(BV_{\text{Band5}}) - 0.4572(BV_{\text{Band7}})$$

The August 1999 scene and the May 2000 scene were so similar that only the August and October, 1999 scenes are discussed here. Because of the ability of the tasseled cap transformation to highlight areas of brightness, wetness, and greenness, it was hypothesized that landslide/debris flow prone areas may show as particularly green. However, landslide/debris flow prone areas were not any different in overall brightness, wetness or greenness. The interesting result of this analysis was that landslides were noticeably brighter in the soil brightness index than surrounding areas. One complication in this analysis is that shadows obscure the actual groundcover and shadow is interpreted as wetness in the analysis.

Layton

In the August 14, 1999 image, the tasseled cap transformation shows the Cedar Bench area to be unusually bright red on the image (possibly the landslide itself, see also Spanish Fork Canyon in this same section) (Figure 55). The South Weber Drive landslide appears green like the rest of the slope. The Heather Drive, Sunset Drive and South Fork Kays Creek slides are all in areas of green and brown, which is a mix of red

and green. Brown is interpreted as dead vegetation and fire damage, based on a small burned area near Hobbs Canyon. In the October 17, 1999 image, the only landslide-prone area that looks appreciably different is Cedar Bench where the brightness is less pronounced and greenness seems to have subdued it (Figure 56). Overall, the entire scene shows a noticeable drop in greenness that is expected between August and October.

Alpine

In the August 14, 1999 scene, Preston and Willow Canyons appear nearly identical (Figure 57). They share the same combination of blue (in this case, shadow is being interpreted incorrectly as wetness) and green. The heads of each canyon are similar. The large red/bright area on the south side of Point of the Mountain is an extensive gravel mining operation.

In the October 17, 1999 scene, overall greenness has decreased, as would be expected. Again, Preston and Willow Canyons share a lot of the same characteristics, the same amount of greenness and yellow/redness (Figure 58).

Spanish Fork Canyon

In the August 14, 1999 scene, Shurtz Lake and Thistle landslide stand out very clearly as bright red areas (Figure 59). This result is unique to this area as that in no other area are the actual landslides as readily apparent. The distribution of greenness in the study area between Shurtz Lake and Thistle landslides is not remarkable. Neither are there any noticeable differences between distributions and intensities of greenness in

Sterling Hollow when compared to Joes Canyon. In the October 17, 1999 scene, the area is noticeably less green but that decrease in greenness is uniform, expected, and not localized in any way (Figure 60).

Santaquin

Tributary 4 has a single drainage of brightness not comparable to anything in Tributary 5 for the August 14, 1999 tasseled cap transformation (Figure 61). Both canyons have the same characteristics but these characteristics are not distinctive from those found in the surrounding canyons. Tributaries 4 and 5 have similar mixes of greenness and brightness as nearby canyons.

In the October 17, 1999 scene, the areas of brightness are more readily apparent but Tributaries 4 and 5 do not look significantly different than surrounding canyons (Figure 62). Tributary 4 canyon has some streaks of brightness that are unique. The debris flows could have been triggered by a condition that existed before the 2001 Mollie Fire but this is inconclusive because these scenes pre-date that event.

CONCLUSIONS

Change detection using the Normalized Difference Vegetation Index (NDVI) showed no correlation between areas that showed no change in NDVI between August and October. The landslide/debris flow prone areas showed the changes that would be expected as plants died off in the fall but these changes were similar to surrounding areas that were not presumed to be landslide/debris flow prone. Change detection using band 5 showed that Thistle and Shurtz Lake landslides changed differently than the surrounding, landslide-prone areas. Some unique surface conditions must exist in these two landslides. The tasseled cap transformation showed that landslides, particularly the Thistle, Shurtz Lake and possibly Cedar Bench slides are drier than surrounding areas. This may correlate to the changes in band 5 for these areas. Other areas were perhaps too small to draw the same conclusions.

The conclusions made here corroborate the statement made by Sauchyn and Trench (1978) with regards to Landsat 3 – Landsat 7 ETM+ still lacks the spatial resolution necessary to delineate the spectral characteristics of landslide/debris flow prone areas. Although the spatial resolution may be the most obvious limitation, it could be that phenomena for which Landsat 7 cannot compensate
may be the true limiting factors. This includes such auxiliary data as weather, difference in slope, subsurface conditions, or groundwater conditions. Despite improved resolution and more advanced digital image processing software, the fundamental problem remains what it has been for many years –coarse spatial resolution. Until a remote sensing

program is developed with an instrument that covers the same range of the electromagnetic spectrum but with even greater spatial resolution, these spectral characteristics will remain veiled.

Geologists would be well served to continue research into the limitations and benefits of incorporating the vast amount of remote sensing data available into the toolkit used to solve problems. Any future work done on the problem of identifying distinctive surface features of landslide/debris flow prone areas should make several changes. First, selected images should be recent. Only two images are absolutely necessary – one before the landslide/debris flow and one after the event. Also, field work should be done as soon after the event as possible and follow-up field work should be done on the same date as the second (post-event) image. This assures that what the analyst interprets is based on the best possible ground truth data and not on assumptions or conjecture.

REFERENCES

Anderson, J.R., Hardy, E.E., Roach, J.T., and Witmer, R.E., 1976, A Land Use and Land Cover Classification System for Use with Remote Sensor Data, United States Geological Survey, Professional Paper 964, 28 p.

Ashland, F.X., 2003, Characteristics, causes, and implications of the 1998 Wasatch Front landslides, Utah: Utah Geological Survey Special Study.

Ashland, F.X., 2002, Preliminary hazards assessment of the Frontier Drive landslide, Mountain Green, Morgan County, Utah: Utah Geological Survey, Report of Investigation 250, p. 17-28.

Ashland, F.X., 2000, Lessons Learned from the 1998 Wasatch Front Landslides: Utah Geological Survey Notes, v. 32, p. 1-4.

Ashland, F.X., 1997, Reconnaissance of the Shurtz Lake landslide, Utah County, Utah: Utah Geological Survey, Report of Investigation 234, 22 p.

Baker, A.A. and Crittenden, M.D., Jr., 1961, Geology of the Timpanogos Cave Quadrangle, Utah: United States Geological Survey Map GQ-132.

Black, B.D., 1998, Reconnaissance of a landslide along the Davis-Weber canal near 1250 East South Weber Drive, South Weber, Davis County, Utah; Technical Reports for 1998: Applied Geology Program, Utah Geological Survey, Report 98-13.

Brabb, E.E., Wieczorek, G.F., and Harp, E.L., 1989, Map showing 1983 landslides in Utah; United States Geological Survey, Miscellaneous Field Studies Map I-2085.

Christenson, G.E., 1998, Spring Landslides Keep UGS Busy: Utah Geological Survey Notes, v. 31, p. 6-7.

City of Santaquin, Utah, 2003, http://www.ulct.org/santaquin/

ERDAS, 1999, ERDAS Field Guide: Atlanta –ERDAS, Inc., 698 p.

ERDAS, 2001, ERDAS Tour Guide: Atlanta –ERDAS, Inc., 694 p.

Giraud, R.E., 2002a, Movement history and preliminary hazard assessment of the Heather Drive landslide, County, Utah: Utah Geological Survey, Report of Investigation 251, 22 p.

Giraud, R.E., 2002b, Landslide Damaged Six Layton Homes: Utah Geological Survey Notes, v. 34, p. 6-7.

Giraud, R.E., 2002c, Map of Alpine mudslides; unpublished – given to M.A. Mabey.

Giraud, R.E., 1998a, Reconnaissance of a landslide on East Sunset Drive, Layton, Davis County, Utah; Technical Reports for 1998: Applied Geology Program, Utah Geological Survey, Report 98-21.

Giraud, R.E., 1998b, Reconnaissance of a landslide on South Fork Kays Creek, Layton, Davis County, Utah; Technical Reports for 1998: Applied Geology Program, Utah Geological Survey, Report 98-21.

Hardy, R.L., 2002a, Mud engulfs homes: Deseret News, September 13, 2002.

Hardy, R.L., 2002b, Slide site described as 'debris flow area': Deseret News, September 17, 2002.

Hardy, R.L., 2001, Santaquin fears a mudslide; Flooding likely from hillsides scorched by fire: Deseret News, October 16, 2001.

Harty, K.M., 1991, Landslide Map of Utah: Utah Geological and Mineralogical Survey, Map 133.

Jensen, J.R., 1996, Introductory Digital Image Processing: Prentice Hall, 318 p.

Jensen, J.R., 2000, Remote Sensing of the Environment: Prentice Hall, 541 p.

Kaliser, B.N. and Slosson, J.E., 1988, Geologic consequences of the 1983 wet year in Utah: Utah Geological and Mineral Survey, Miscellaneous Publication 88-3.

Kauth, R.J. and Tomas, G.S., 1976, The tasseled cap – a graphic description of the spectral-temporal development of agricultural crop as seen by Landsat: Symposium on Machine Processing of Remotely Sensed Data, June 29- July 1, 1976, the Laboratory for Applications of Remote Sensing, Purdue University, West Lafayette, Indiana, Proceedings, p. 4B-41 – 51.

Machette, M. N., 1992, Surficial Geologic Map of the Wasatch Fault Zone, Eastern part of Utah Valley, Utah County and parts of Salt Lake and Juab counties, Utah: United States Geological Survey, Map I-2095.

Mantovani, F., Soeters, R., and Van Westen, C.J., 1996, Remote sensing techniques for landslide studies and hazard zonation in Europe: Geomorphology, v. 15, p. 213-225.

McDonald, G.N. and Giraud, R.E., 2002, September 12, 2002, fire-related debris flows east of Santaquin and Spring Lake, Utah County, Utah: Utah Geological Survey, Report No. 02-09

McKean, J., Buechel, S., and Gaydos, L., 1991, Remote Sensing and Landslide Hazard Assessment: Photogrammetric Engineering and Remote Sensing, v. 57, p. 1185-1193.

National Weather Service – Weather Forecast Office Salt Lake City, 2003, http://www.wrh.noaa.gov/Saltlake/climate/normals.1971-2000.slc.shtml

Samarakoon, L., Ogawa, S., Ebisu, N., Lapitan, R., and Kohki, Z., 1993, Inference of landslide susceptible areas by Landsat Thematic Mapper data: IAHS Publ. no. 217.

Sauchyn, D.J. and Trench, N. R., 1978, Landsat Applied to Landslide Mapping: Photogrammetric Engineering and Remote Sensing, v. 44, p. 735-741.

Sheffner, E., 1999, Landsat Program: Ames Research Center http://geo.arc.nasa.gov/sge/landsat/landsat.html

Shih, S.F. and Jordan, J.D., 1993, Use of Landsat Thermal-IR data and GIS in soil moisture assessment: Journal of Irrigation and Drainage Engineering, v. 119, p. 868-879.

Singhroy, V., Mattar, K.E., and Gray, A.L., 1998, Landslide characteristics in Canada using interferometric SAR and combined SAR and TM images: Advances in Space Research, v. 21, p.465-476.

Solomon, B.J., 1998, Reconnaissance of a landslide near the Cedar Bench subdivision, South Weber, Utah; Technical Reports for 1998: Applied Geology Program, Utah Geological Survey, Report 98-14.

U.S. Forest Service, 2001, Initial burned-area emergency rehabilitation (BAER) report for the Mollie fire incident: Unpublished Uinta National Forest report for the Mollie fire incident.

Warnock, C., 2002, Storm hits home: Alpine family affected by mudslide; Daily Herald (Provo, UT), September 8, 2002, p. A3

Witkind, I.J. and Page, W.R., 1983, Geologic Map of the Thistle Area, Utah County, Utah: Utah Geological and Mineral Survey, Map 69.

Witkind, I.J. and Weiss, M.P., 1991, Geologic Map of the Nephi 30’ x 60’ quadrangle, Carbon, Emery, Juab, Sanpete, Utah and Wasatch counties, Utah: United States Geological Survey, I-1937.

Figure 1: Landsat-7 ETM+ subset image of Utah Valley, May 28, 2000. Near infrared (band 4) shown in the red plane, red (band 3) shown in the green plane and green plane and green (band 2) shown in the blue plane.

Figure 2: The study areas for this research - Landsat 7 scene, path 38, row 32, May 28, 2000. The image is displayed as 7, 4, 2; middle infrared (band 7) in the red plane, near infrared (band 4) in the green plane and green (band 2) in the blue plane. The four study areas are marked.

Figure 3: Landslides (1998-2001) of the Layton and South Weber area. The image was taken on May 28, 2000 and is displayed as bands 4, 3, 2.

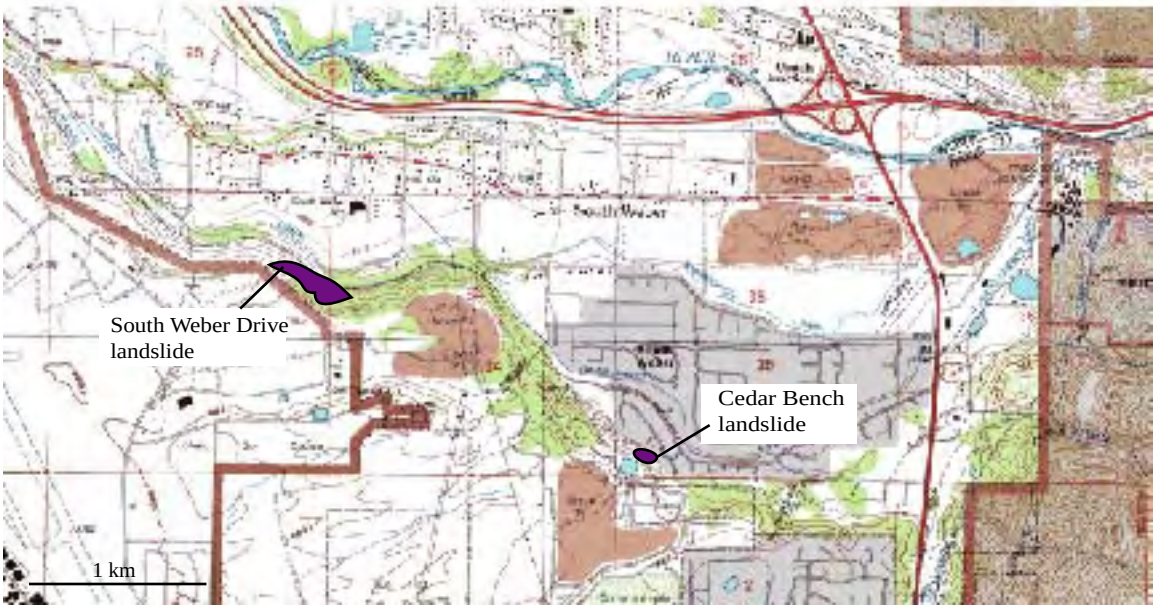

Figure 4: Topographic map of the location, morphology, and slope of the South Weber area landslides.

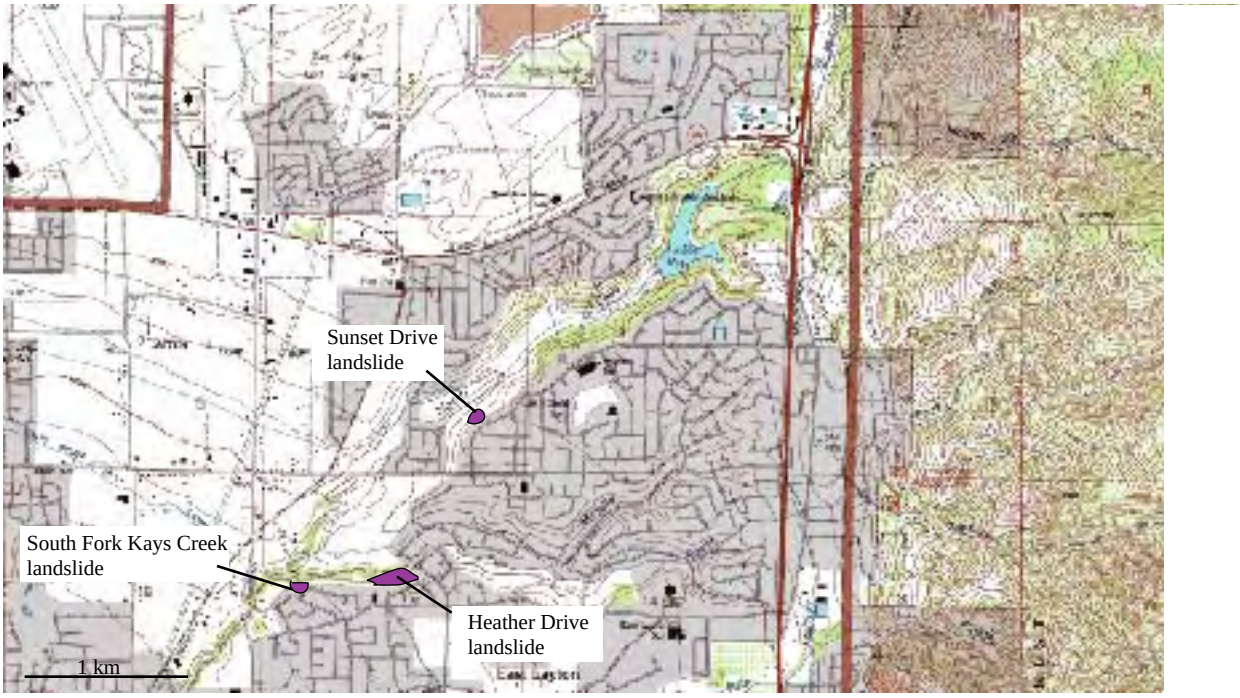

Figure 5: Topographic map showing the location, morphology and slope of the Layton area landslides.

Figure 6: The Heather Drive landslide; houses remaining on Heather Drive are visible at the top of the bluff. The landslide itself is mostly revegetated and not clearly visible.(August 2002)

Figure 7: The South Weber Drive landslide visible as small scarps in the slope. (July 2002)

Figure 8: The September 8 Preston Canyon debris flow where it crossed Preston Canyon Drive; Preston Canyon is visible in the background. Photograph taken facing east. (September 18, 2002)

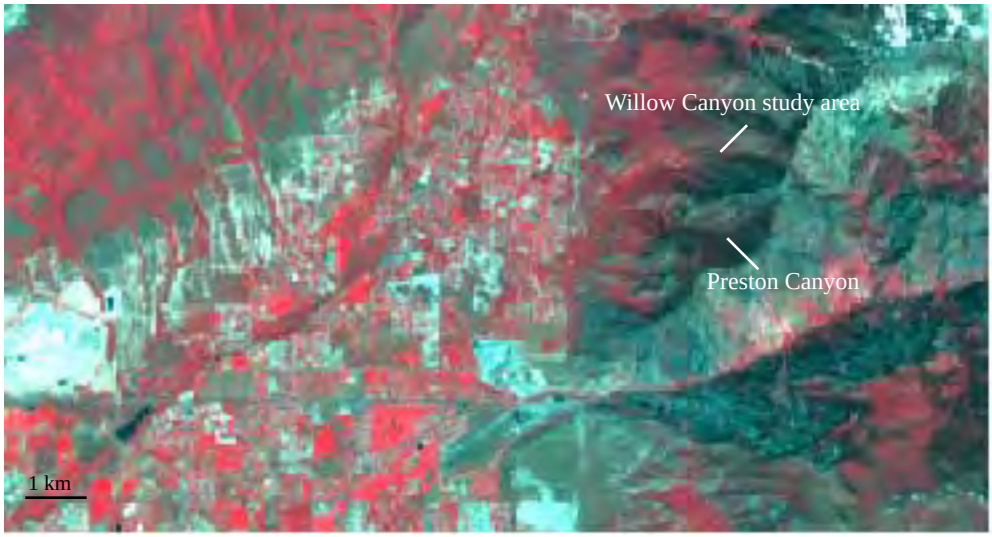

Figure 9: Locations of Preston and Willow Canyons in Alpine area; Landsat 7 scene using bands 4, 3 and 2 (May 28, 2000).

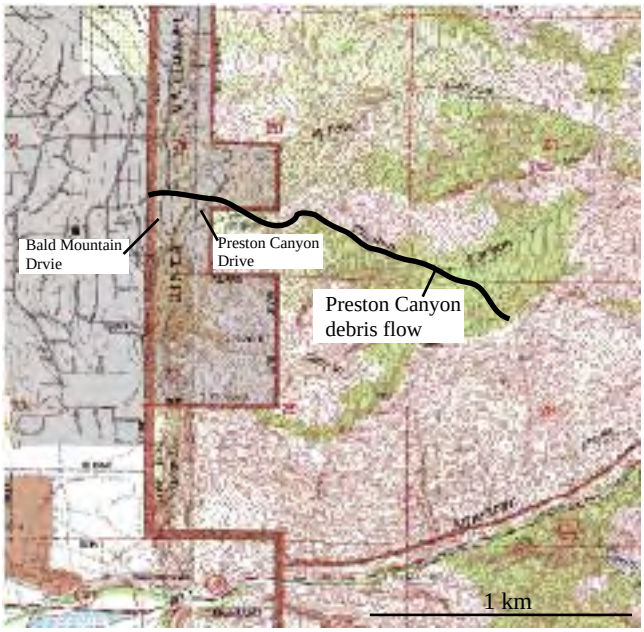

Figure 10: Topographic map showing location of the Preston Canyon debris flow and affected areas.

Figure 11: Preston Canyon Drive where the debris flow crossed Bald Mountain Drive, photograph taken facing east. (September 18, 2002)

Figure 12: The channel of the Preston Canyon debris flow, photograph taken facing east. (September 18, 2002)

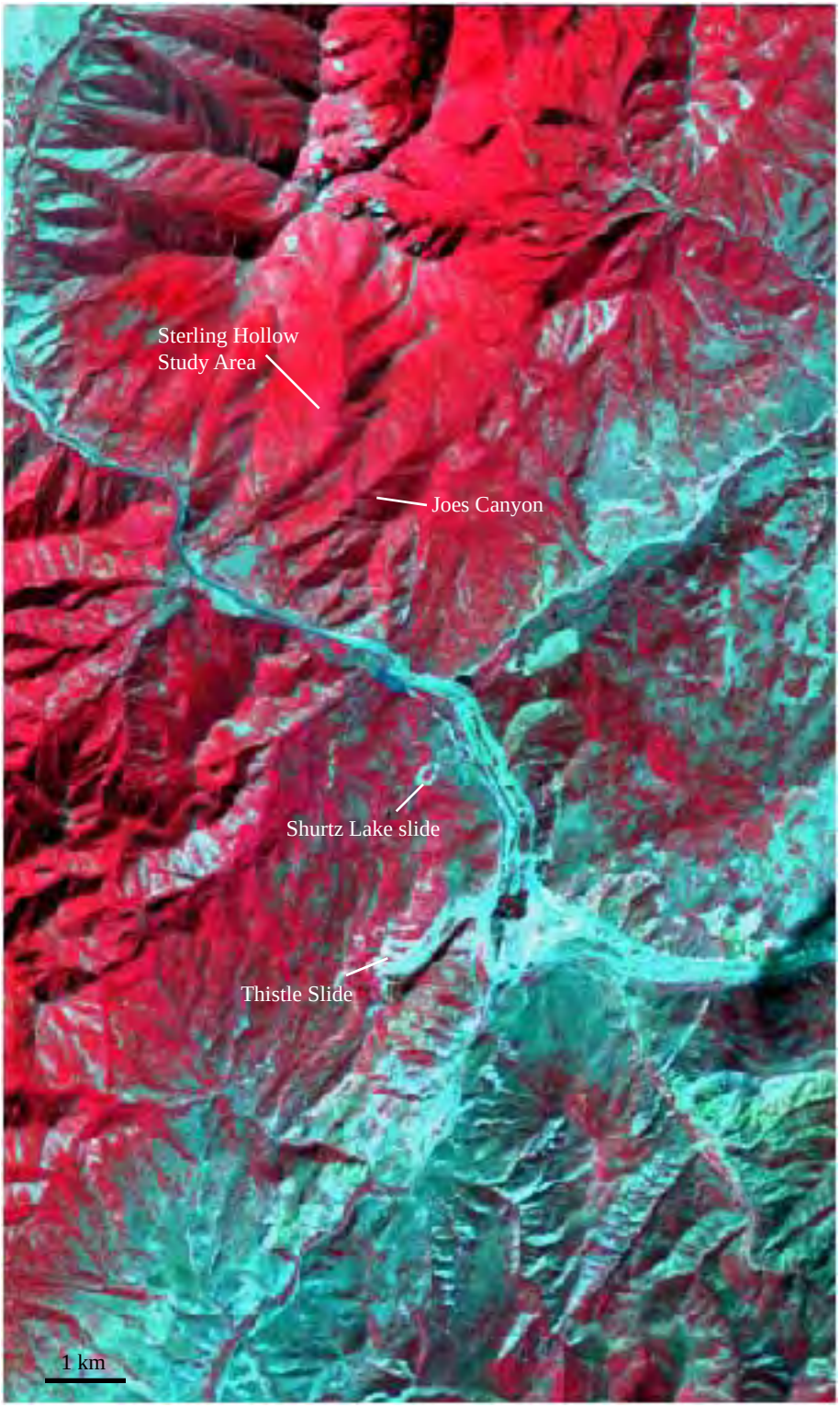

Figure 13: Location of landslides and debris flows in Spanish Fork Canyon. Landsat 7 subset, bands 4, 3,2; imaged May 28, 2000.

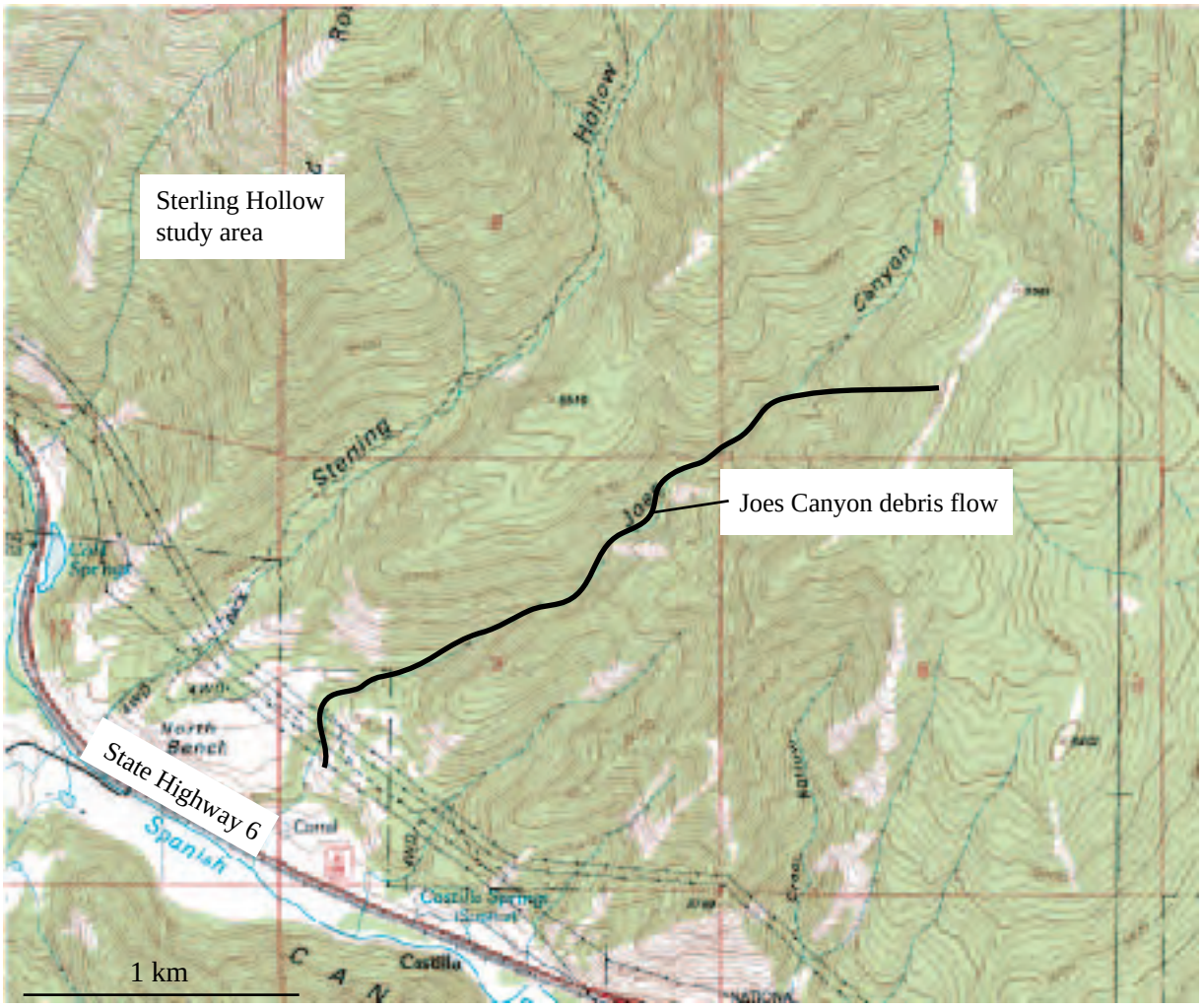

Figure 14: Topographic map of Sterling Hollow and Joes Canyon, and path of Joes Canyon debris flow.

Figure 15: Topographic map of the locations and morphology of the Thistle slide and Shurtz Lake landslide.

Figure 16: Thistle landslide, photograph taken facing southwest. (July 4, 2002)

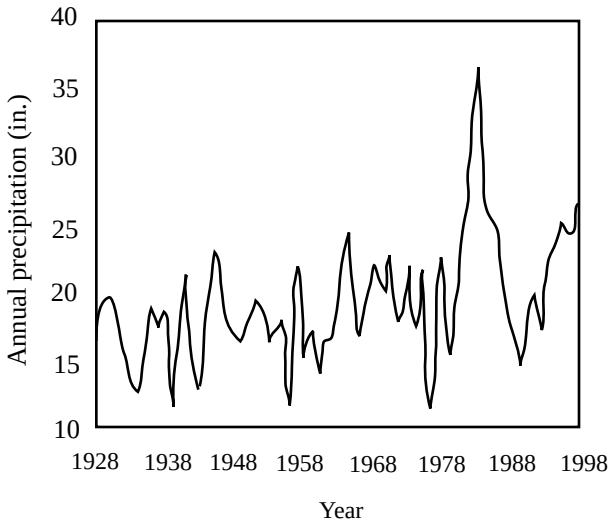

Figure 17: Precipitation curve for Spanish Fork Canyon, 1928-1998; Ashland, 1998.

Figure 18: Shurtz landslide, photograph taken facing west. Only the two earthflows are visible, the remainder of the slide is on the plateau. (July 4, 2002)

Figure 19: The channel of Joes Canyon debris flow, photograph taken facing south-southwest. (July 4, 2002)

Figure 20: Levee of Joes Canyon debris flow, photograph taken facing south. (July 4, 2002)

Figure 21: Toe of the Joes Canyon debris flow fan, photograph taken facing north. Jared Howland in foreground. (July 4, 2002)

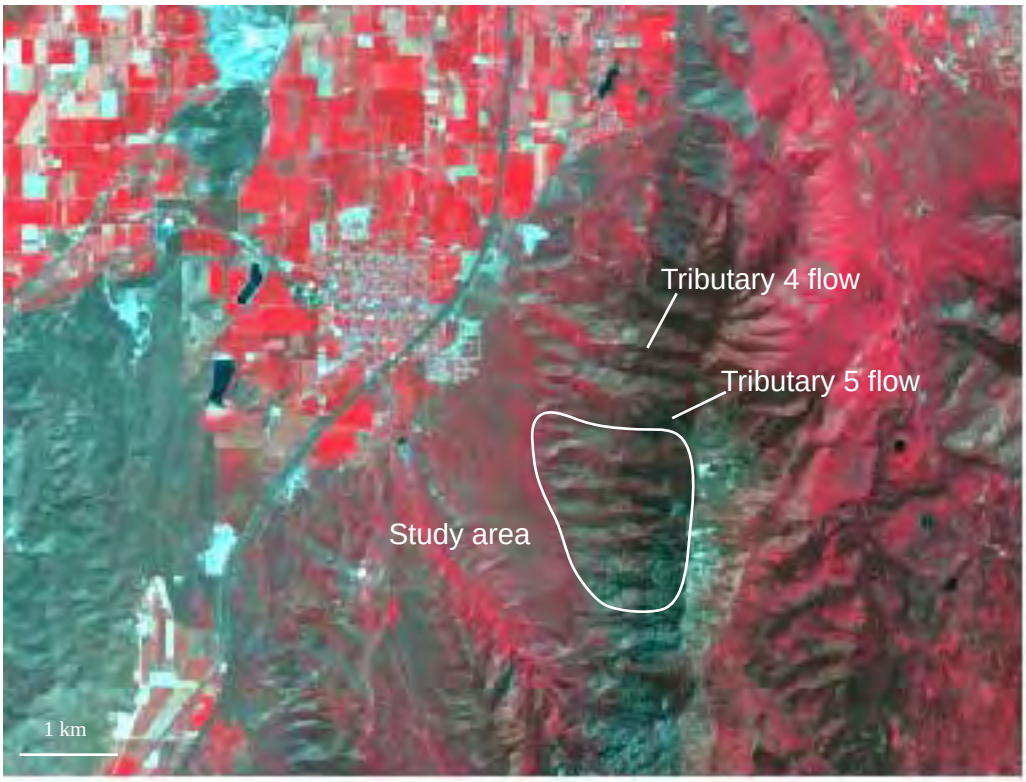

Figure 22: Locations of Tributaries 4 and 5 flows and study area for Santaquin; Landsat 7 scene using bands 4, 3 and 2, imaged May 28, 2000.

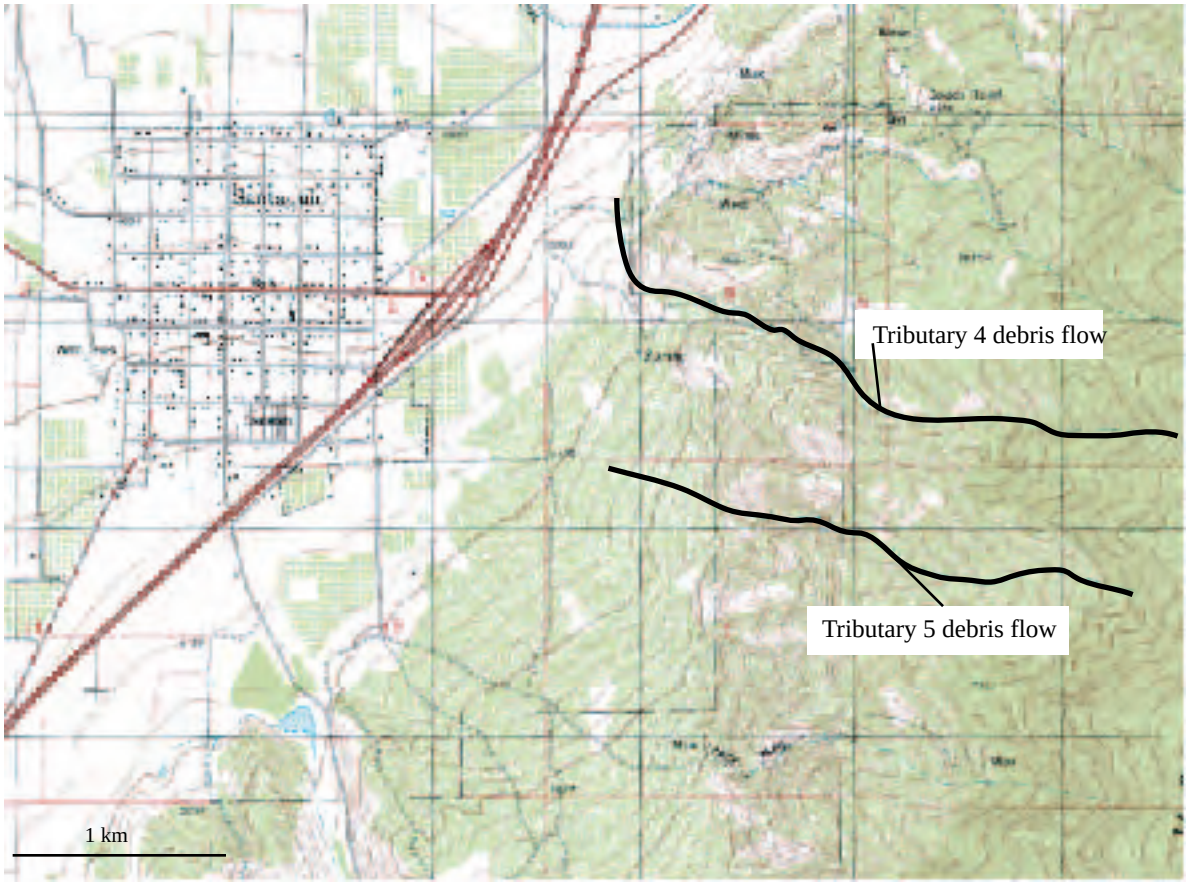

Figure 23: Topographic map showing locations of Tributary 4 and 5 debris flows and affected areas. The subdivision hit by the Tributary 4 debris flow is not shown on this map.

Figure 24: Source area of the Tributary 5 debris flow, photograph taken facing south. Note the burned trees from the Mollie Fire in 2001. (September 19, 2002)

Figure 25: The Tributary 4 debris flow and the subdivision it hit, photograph taken facing northwest. (September 19, 2002)

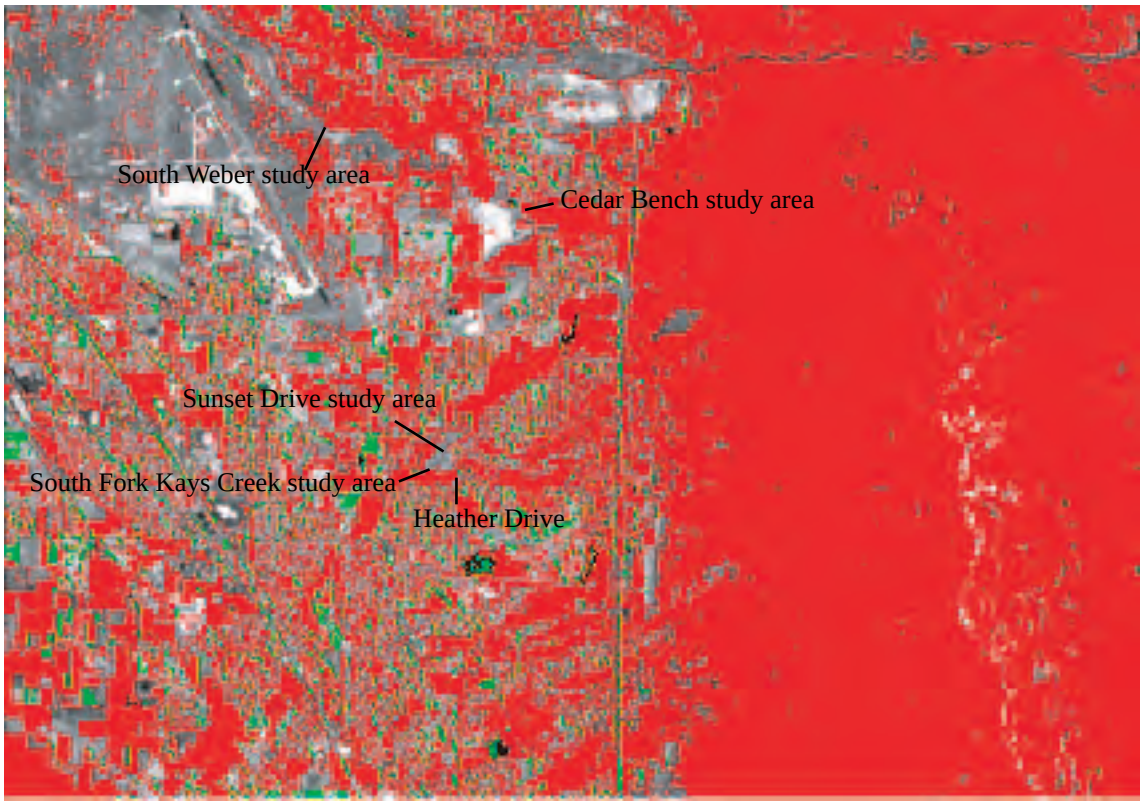

Figure 26: Layton subset scene (band 8) overlain by areas of +/- 5% change in NDVI between August 14, 1999 and October 17, 1999. Red areas decreases in NDVI of greater than 5% and green areas show increases in NDVI of greater than 5%. The study areas show decreases.

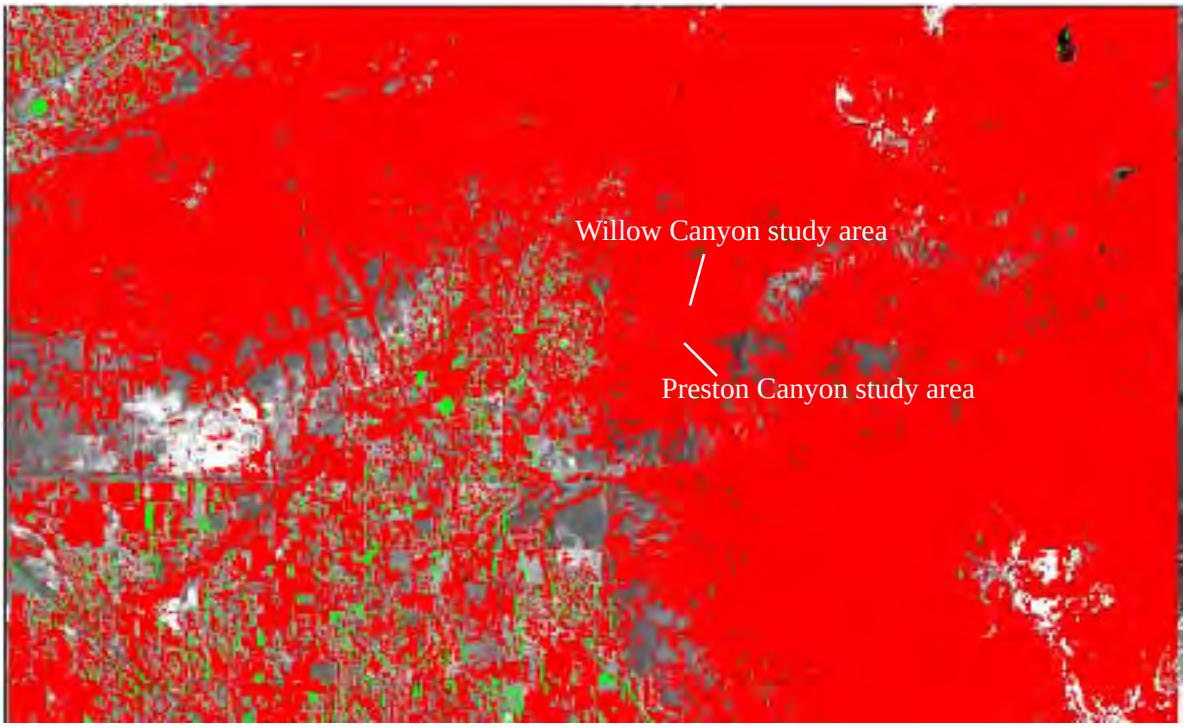

Figure 27: Alpine subset scene (band 8) overlain by areas of +/- 5% change in NDVI between August 14, 1999 and October 17, 1999. Red areas decreases in NDVI of greater than 5% and green areas show increases in NDVI of greater than 5%. The study areas show decreases.

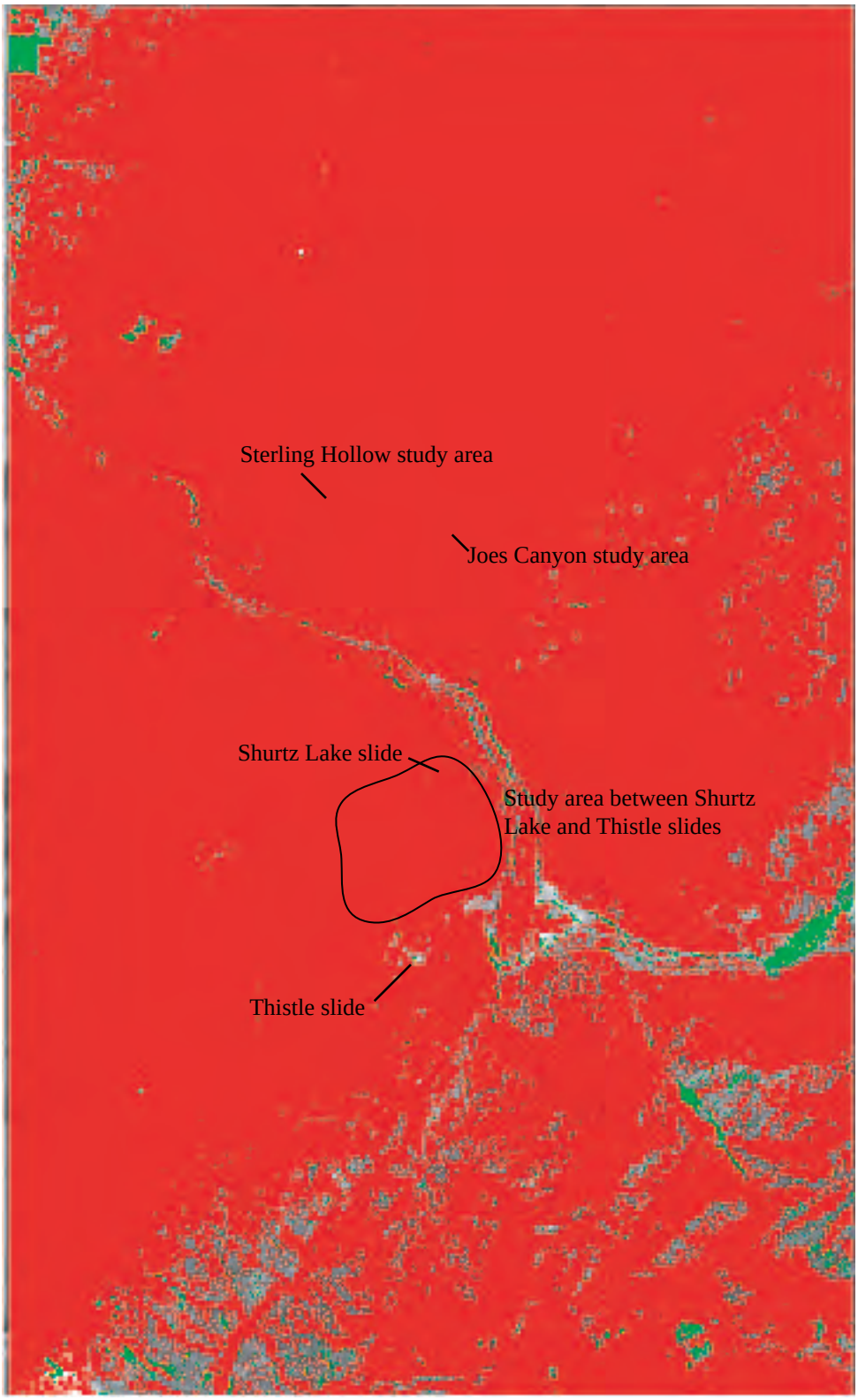

Figure 28: Spanish Fork subset scene (band 8) overlain by areas of +/- 5% change in NDVI between August 14, 1999 and October 17, 1999. Red areas decreases in NDVI of greater than 5% and green areas show increases in NDVI of greater than 5%. The study areas show decreases.

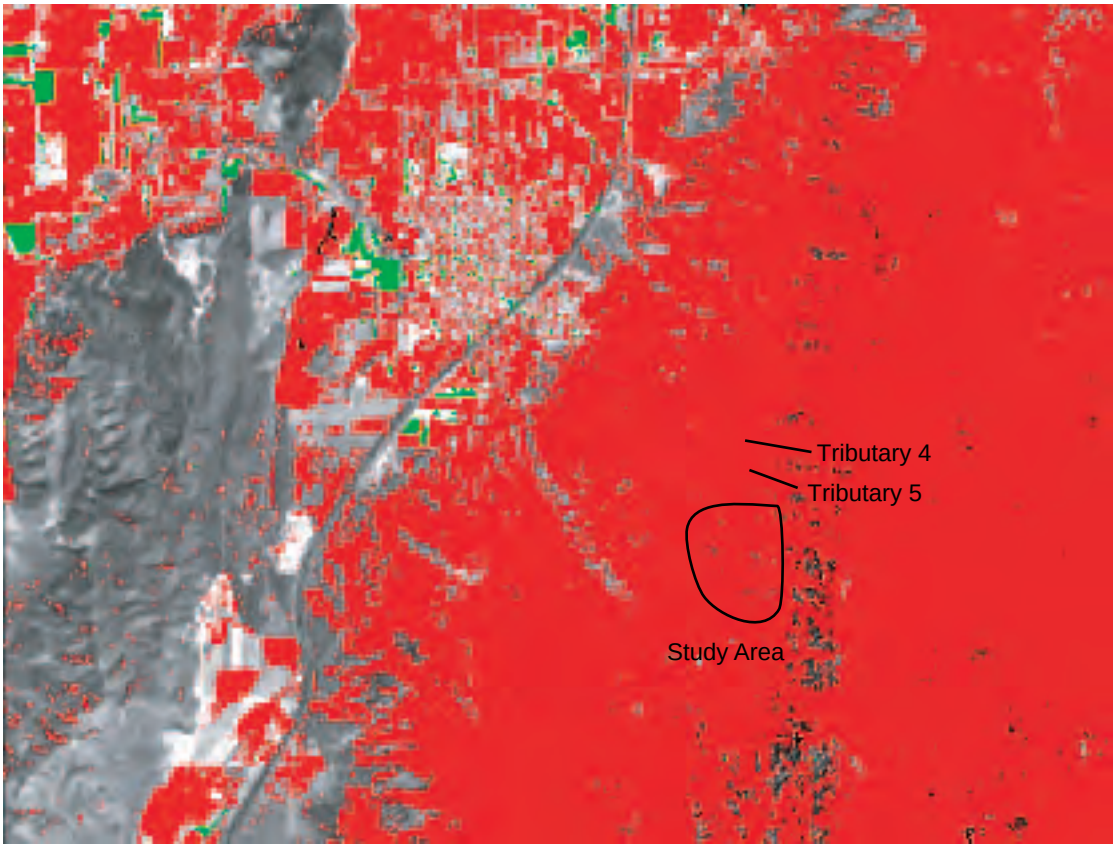

Figure 29: Santaquin subset scene (band 8) overlain by areas of +/- 5% change in NDVI between August 14, 1999 and October 17, 1999. Red areas decreases in NDVI of greater than 5% and green areas show increases in NDVI of greater than 5%. The study areas show decreases.

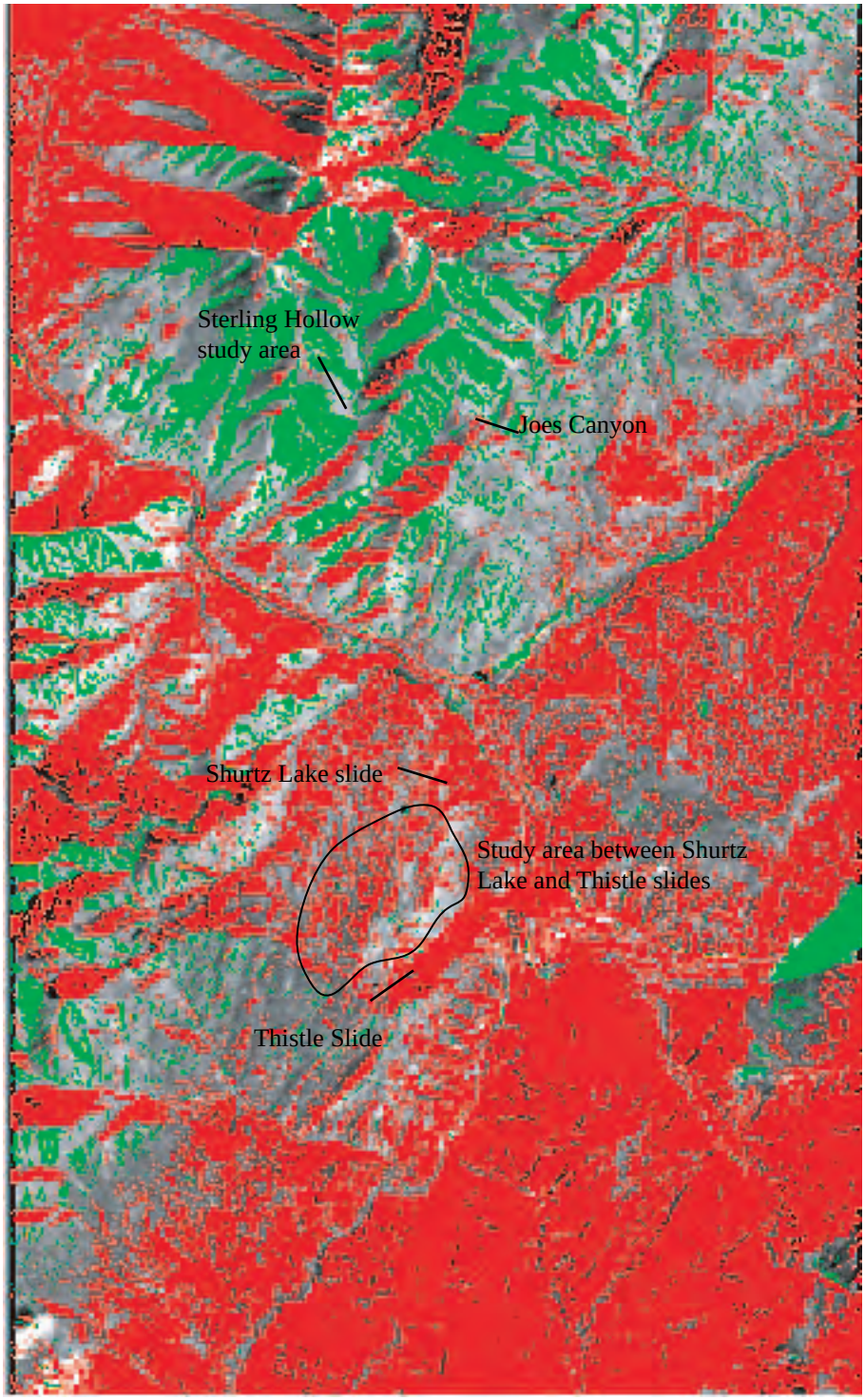

Figure 30: Spanish Fork subset of Landsat 7 scene (band 8) overlain by changes in band 5 between August 14, 1999 and October 17, 1999 at +/- 10% change. Red areas show decreases of greater than 10% and green areas show increases of greater than 10%.

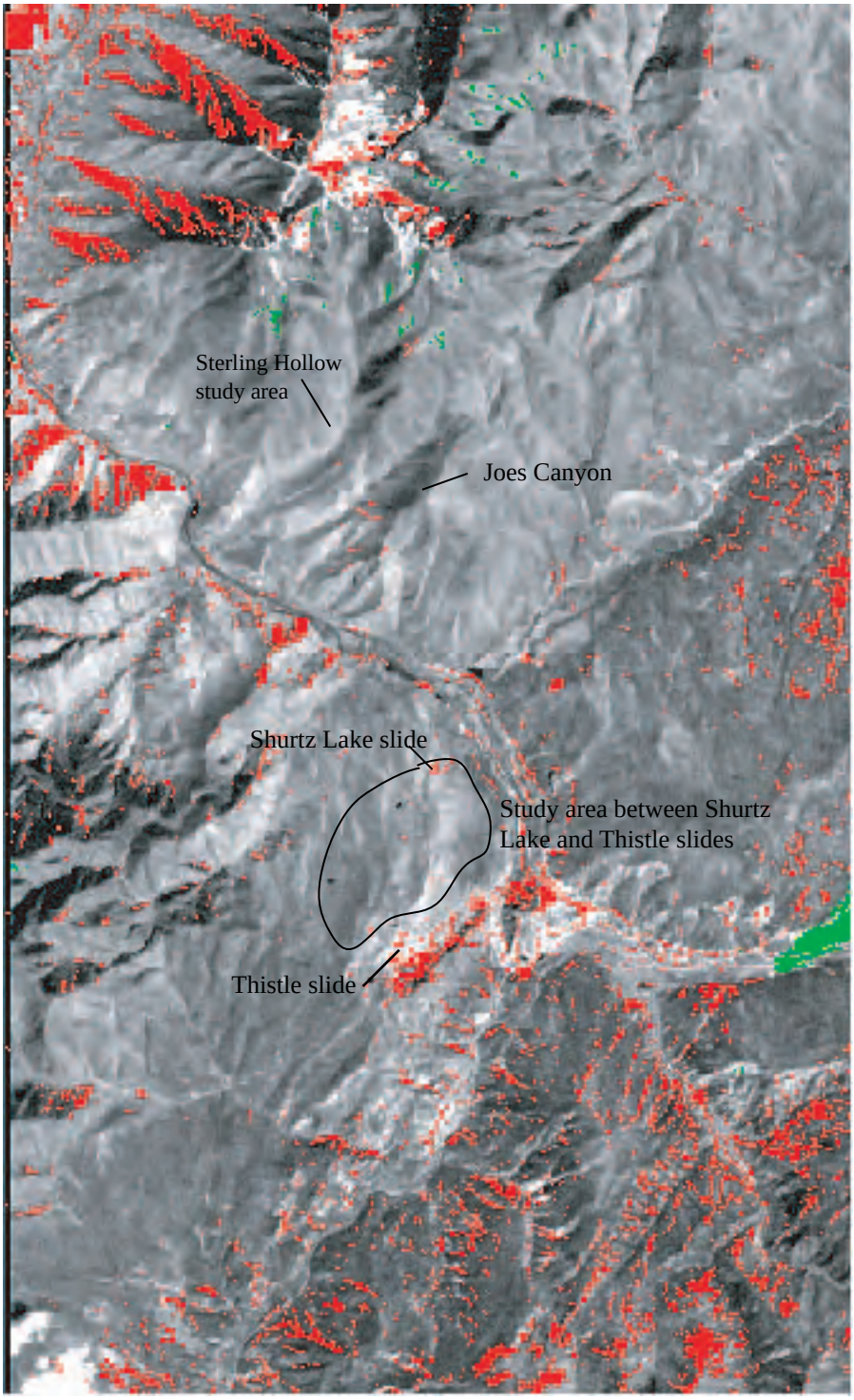

Figure 31: Spanish Fork subset of Landsat 7 scene (band 8) overlain by changes in band 5 between August 14, 1999 and October 17, 1999 at +/- 30% change. Red areas show decreases of greater than 30% and green areas show increases of greater than 30%. There is some concentration of areas of decrease (red) in Shurtz Lake slide and near/in Thistle slide.

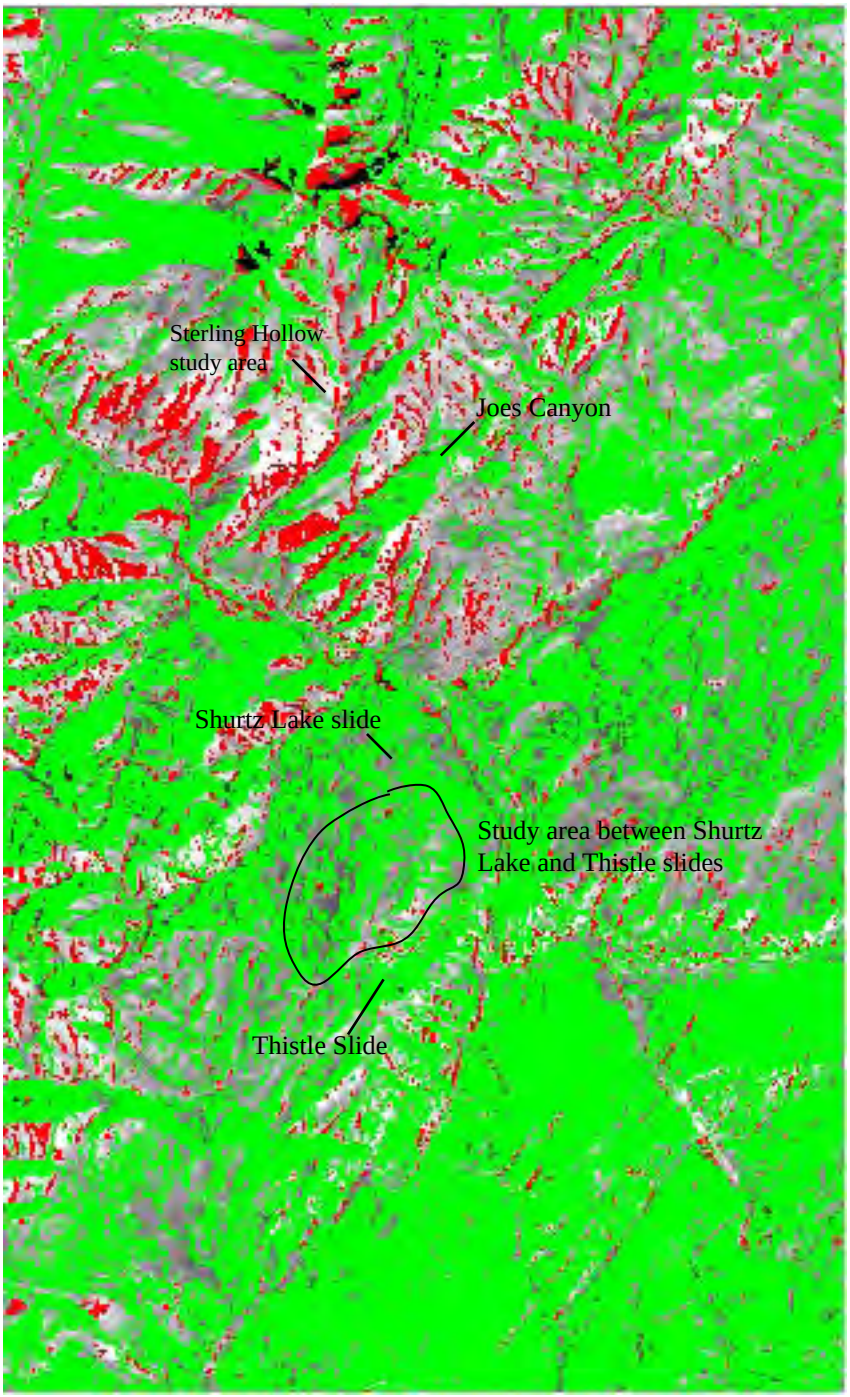

Figure 32: Spanish Fork subset of Landsat 7 scene (band 8) overlain by changes in band 5 between October 17, 1999 and May 28, 2000 at +/- 10% change. Red areas show decreases of greater than 10% and green areas show increases of greater than 10%.

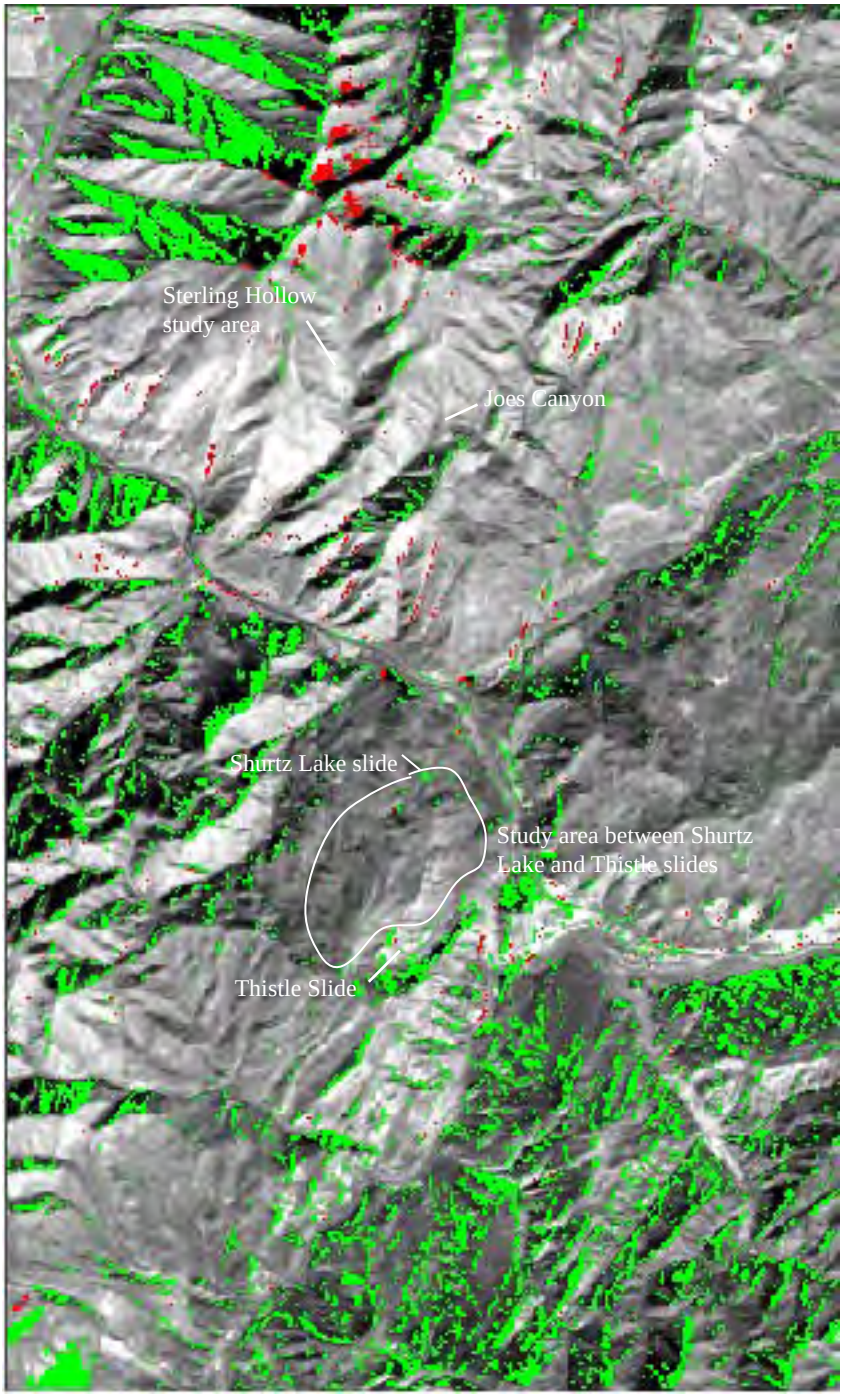

Figure 33: Spanish Fork subset of Landsat 7 scene (band 8) overlain by changes in band 5 between October 17, 1999 and May 28, 2000 at +/- 30% change. Red areas show decreases of greater than 30% and green areas show increases of greater than 30%. There is a concentration of areas of increase (green) for the area near and in Thistle Slide and in the Shurtz Lake slide.

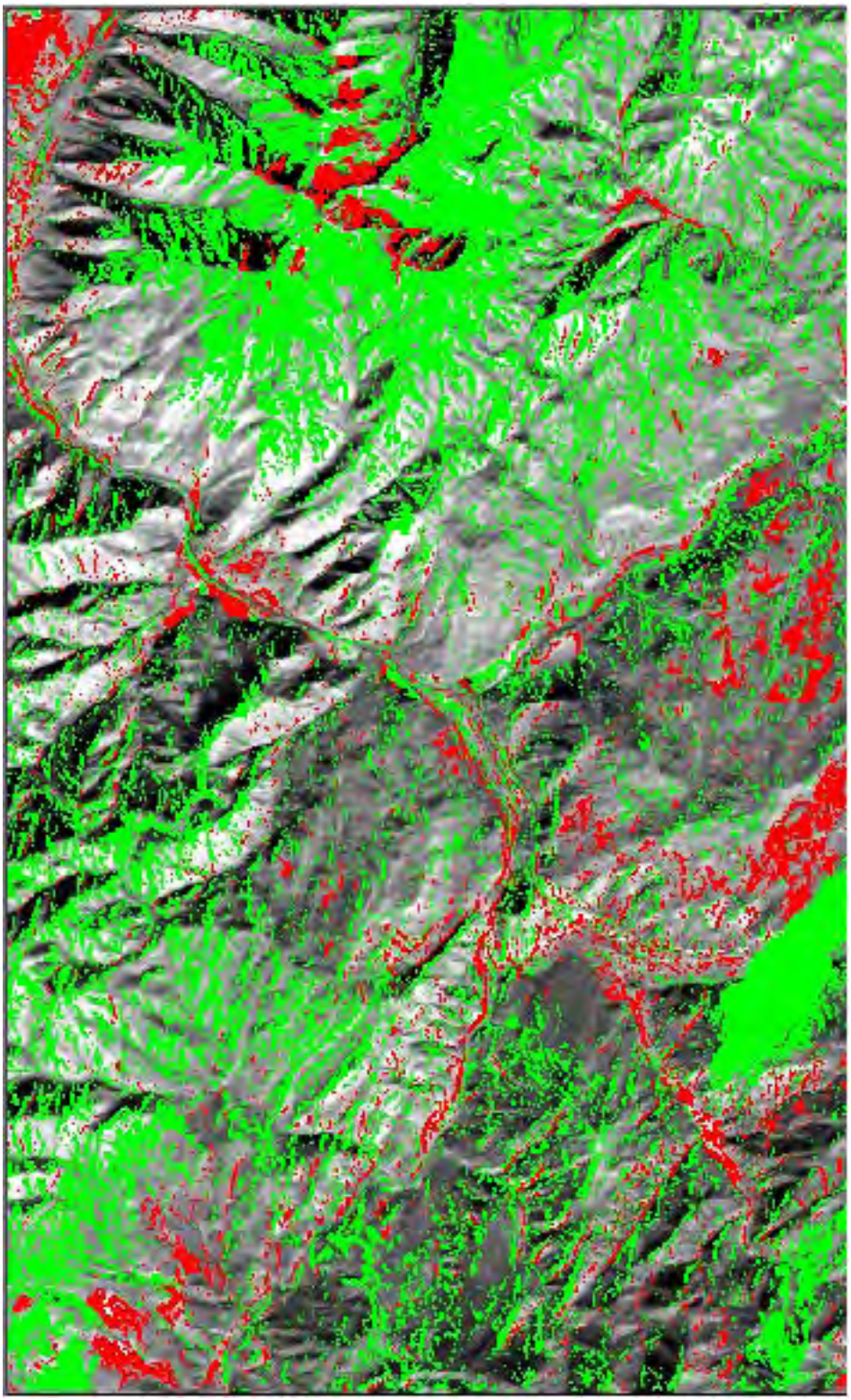

Figure 34: Spanish Fork subset of Landsat 7 scene (band 8) overlain by changes in band 5 between August 14, 1999 and May 28, 2000 at +/- 10% change. Red areas show decreases of greater than 10% and green areas show increases of greater than 10%.

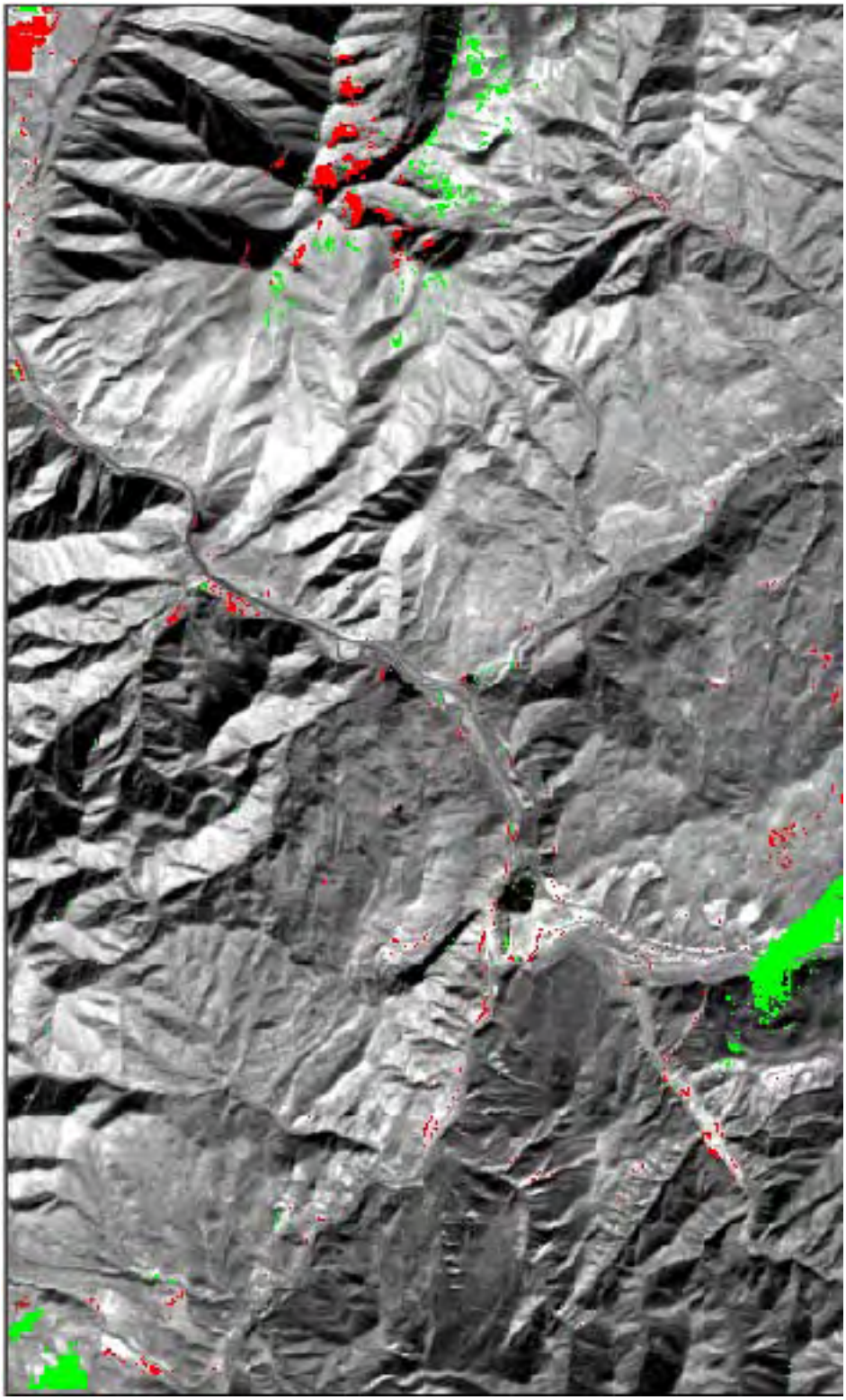

Figure 35: Spanish Fork subset of Landsat 7 scene (band 8) overlain by changes in band 5 between August 14, 1999 and May 28, 2000 at +/- 30% change. Red areas show decreases of greater than 30% and green areas show increases of greater than 30%.

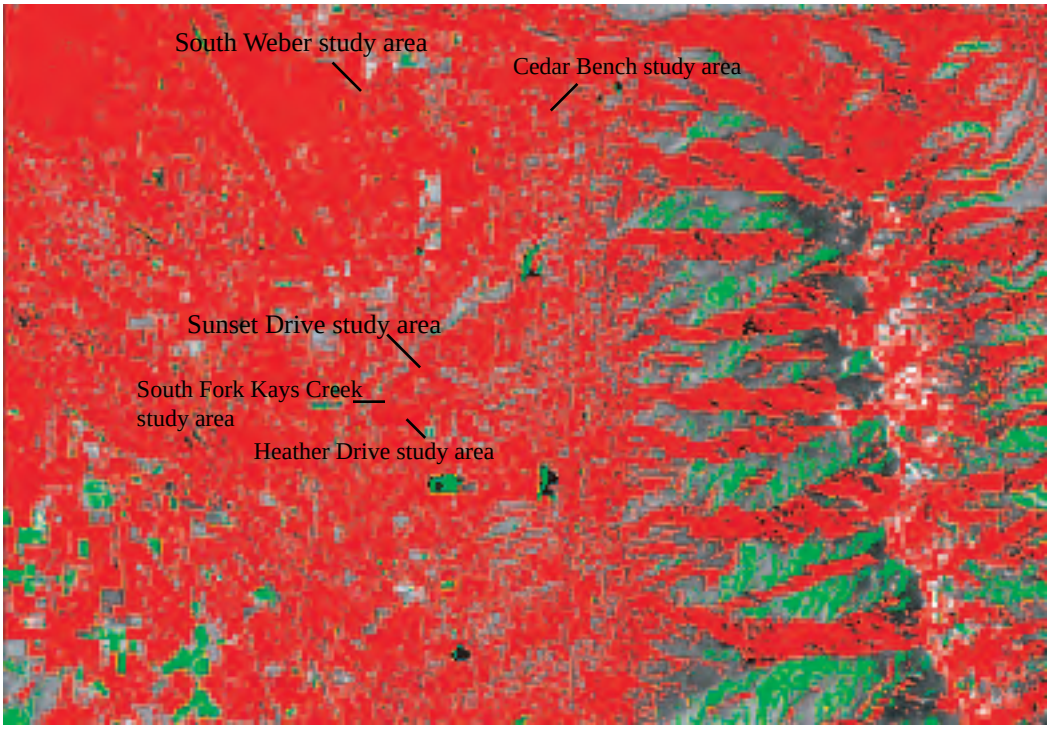

Figure 36: Layton subset of Landsat 7 scene (band 8) overlain by changes in band 5 between August 14, 1999 and October 17, 1999 at +/- 10% change. Red areas show decreases of greater than 10% and green areas show increases of greater than 10%.

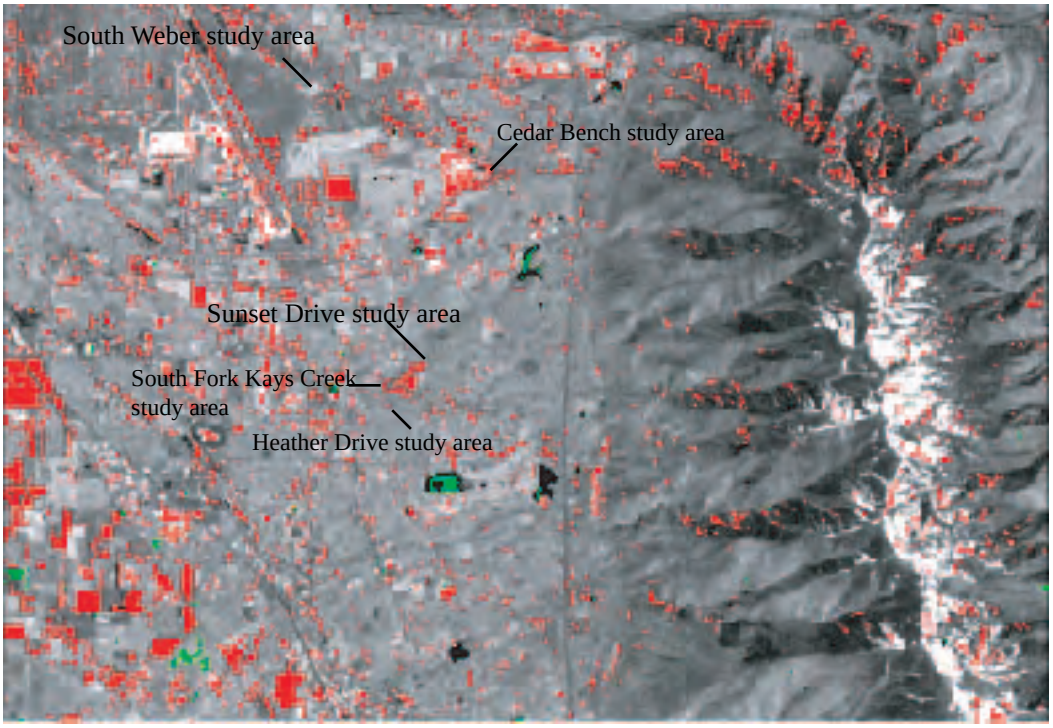

Figure 37: Layton subset of Landsat 7 scene (band 8) overlain by changes in band 5 between August 14, 1999 and October 17, 1999 at +/- 30% change. Red areas show decreases of greater than 30% and green areas show increases of greater than 30%.

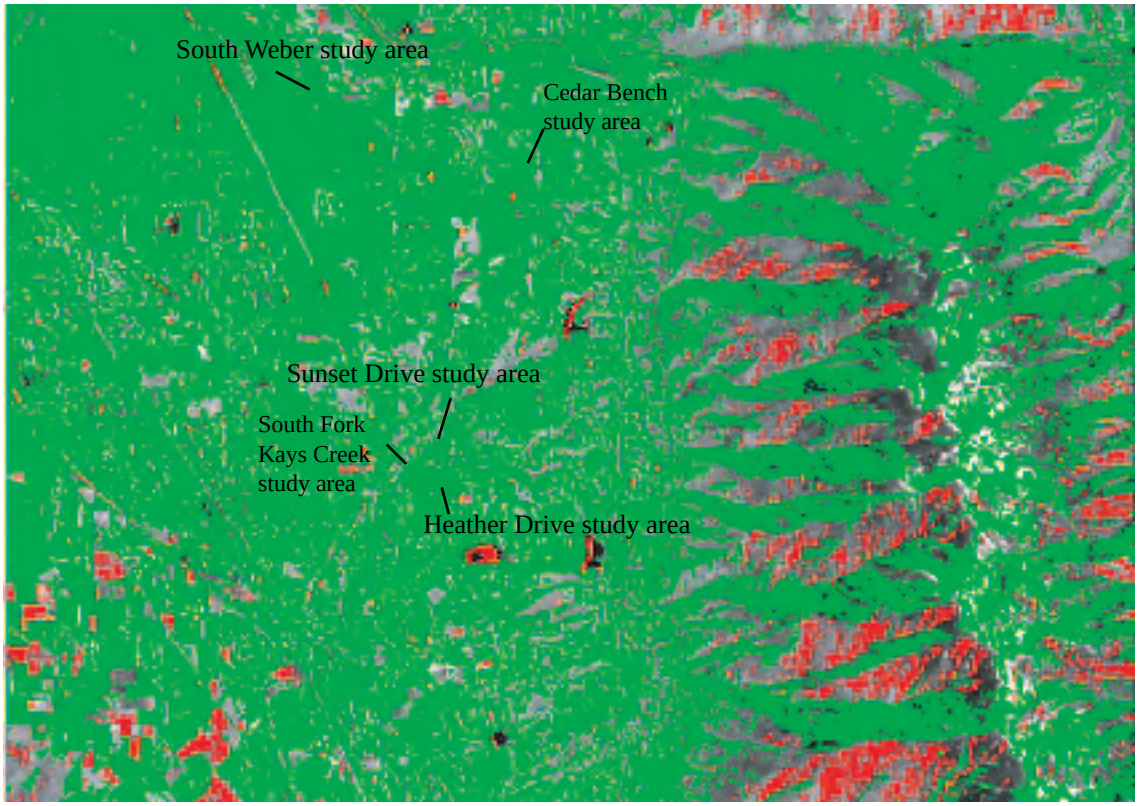

Figure 38: Layton subset of Landsat 7 scene (band 8) overlain by +/- 10% change in band 5 between October 17, 1999 and May 28, 2000. Red shows areas of greater than 10% decrease and green shows areas of greater than 10% increase in brightness value.

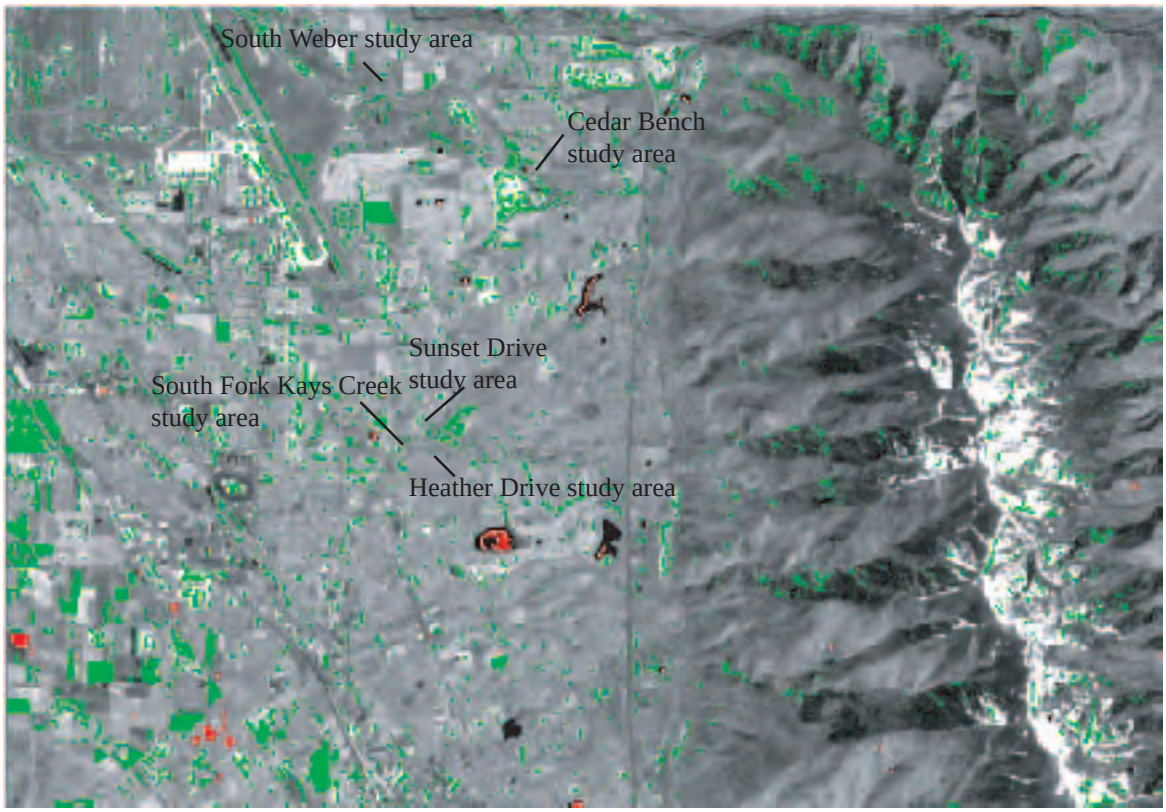

Figure 39: Layton subset of Landsat 7 scene (band 8) overlain by +/- 30% change in band 5 between October 17, 1999 and May 28, 2000. Red shows areas of greater than 30% decrease and green shows areas of greater than 30% increase in brightness value.

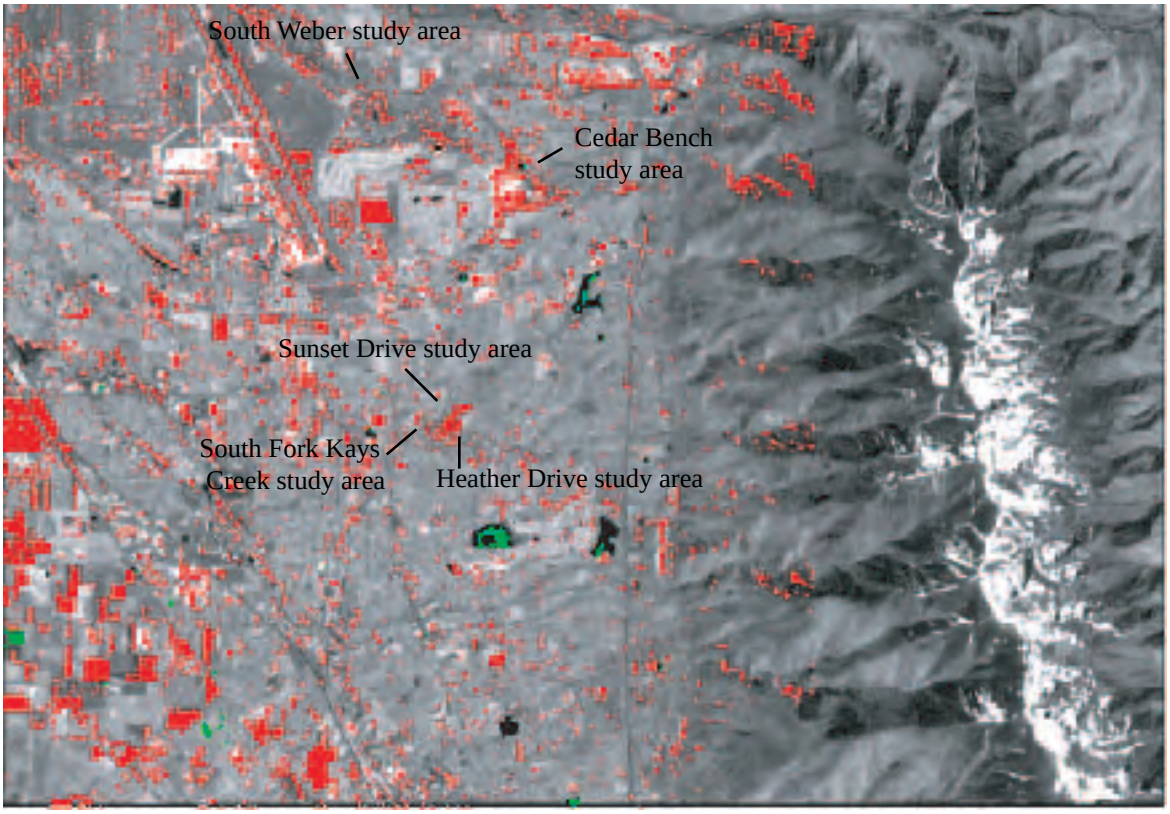

Figure 40: Layton subset of Landsat 7 scene (band 8) overlain by +/- 10% change in band 5 between August 14, 1999 and May 28, 2000. Red shows areas of greater than 10% decrease and green shows areas of greater than 10% increase in brightness value.

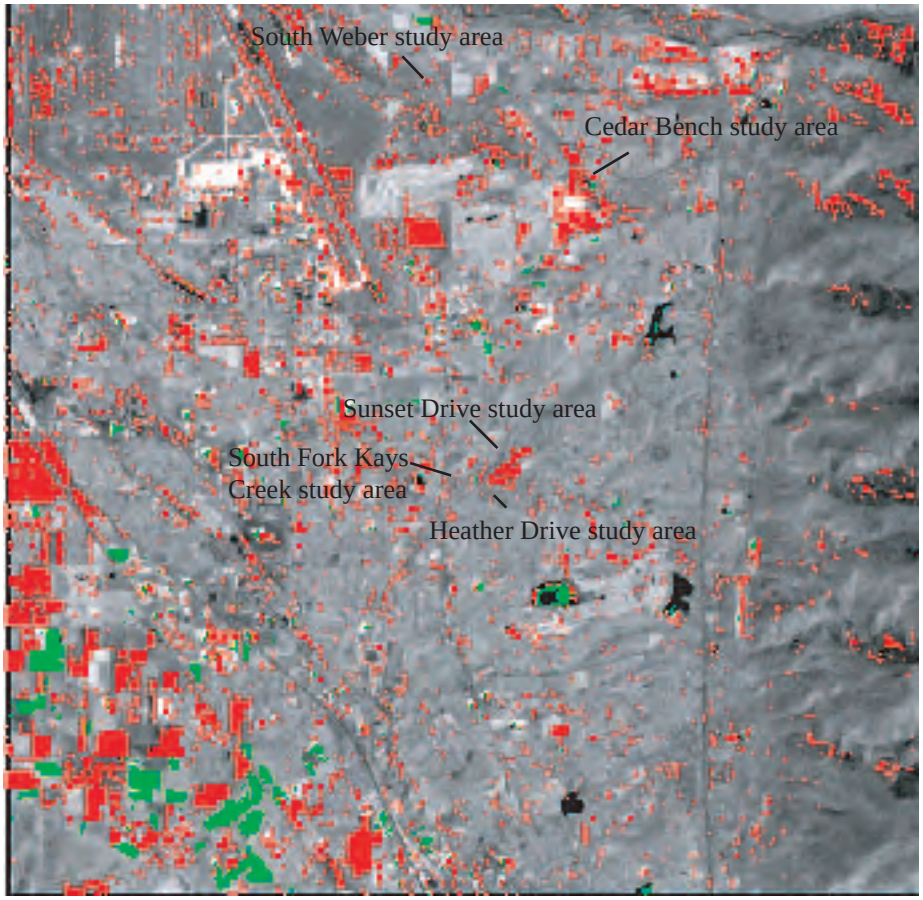

Figure 41: Layton subset of Landsat 7 scene (band 8) overlain by +/- 30% change in band 5 between August 14, 1999 and May 28, 2000. Red shows areas of greater than 30% decrease and green shows areas of greater than 30% increase in brightness value.

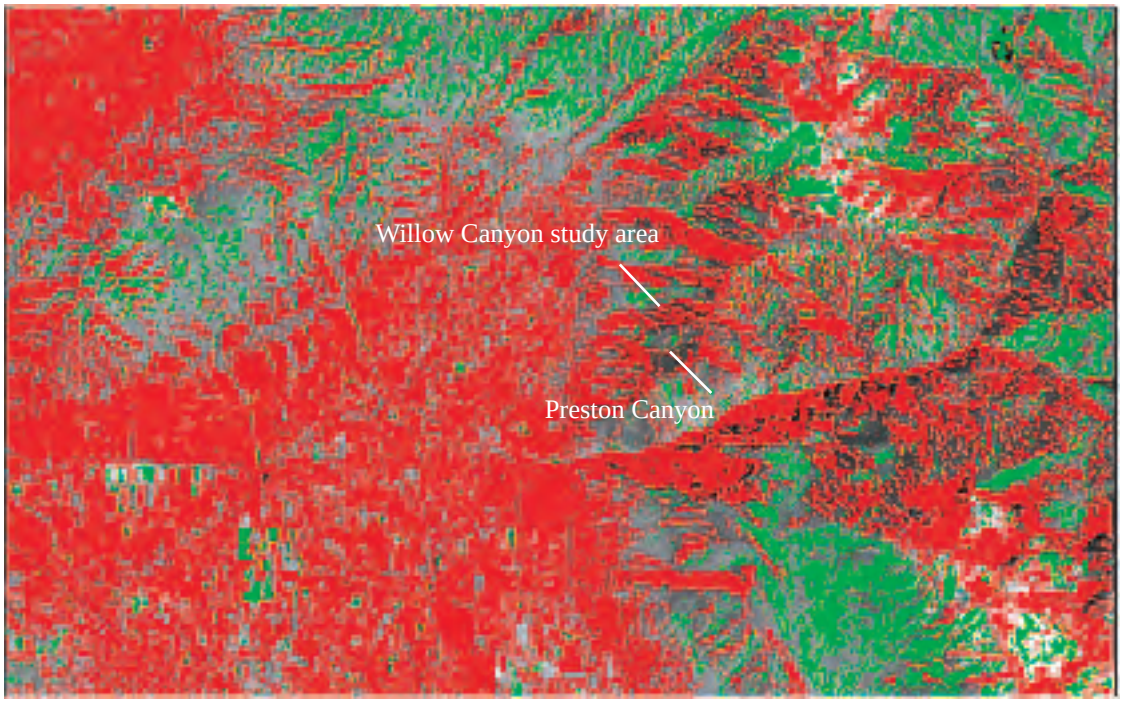

Figure 42: Alpine subset of Landsat 7 scene (band 8) overlain by +/- 10% change in band 5 between August 14, 1999 and October 17. 1999. Red shows areas of greater than 10% decrease and green shows areas of greater than 10% increase in brightness value.

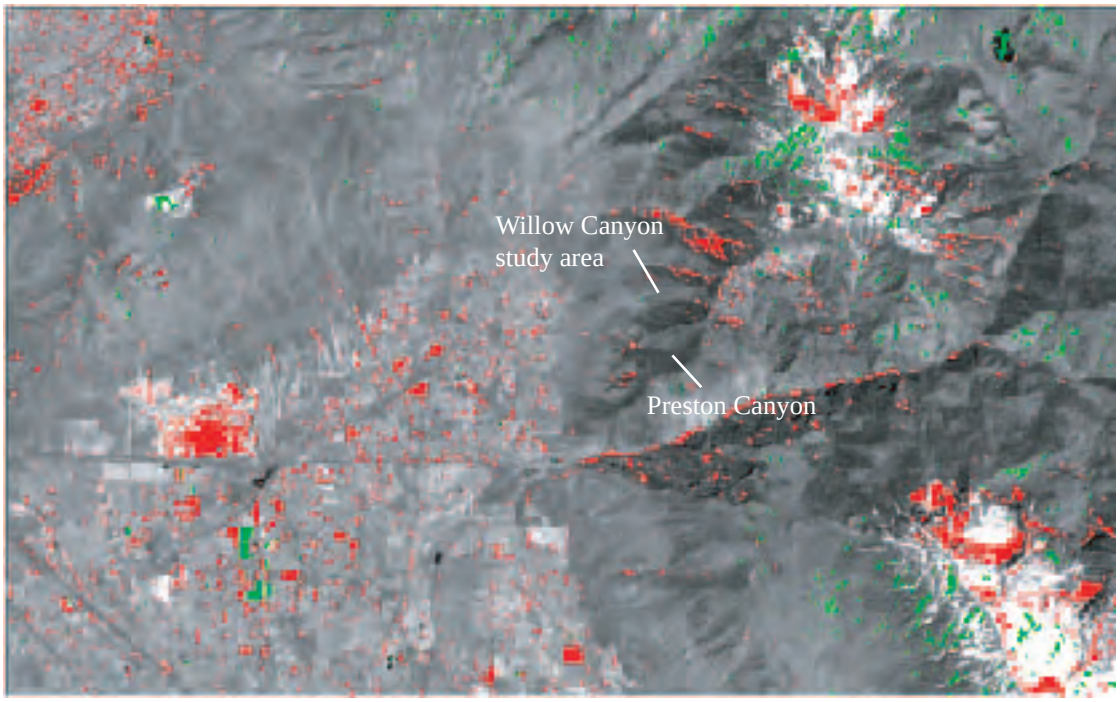

Figure 43: Alpine subset of Landsat 7 scene (band 8) overlain by +/- 10% change in band 5 between August 14, 1999 and October 17. 1999 . Red shows areas of greater than 10% decrease and green shows areas of greater than 10% increase in brightness value.

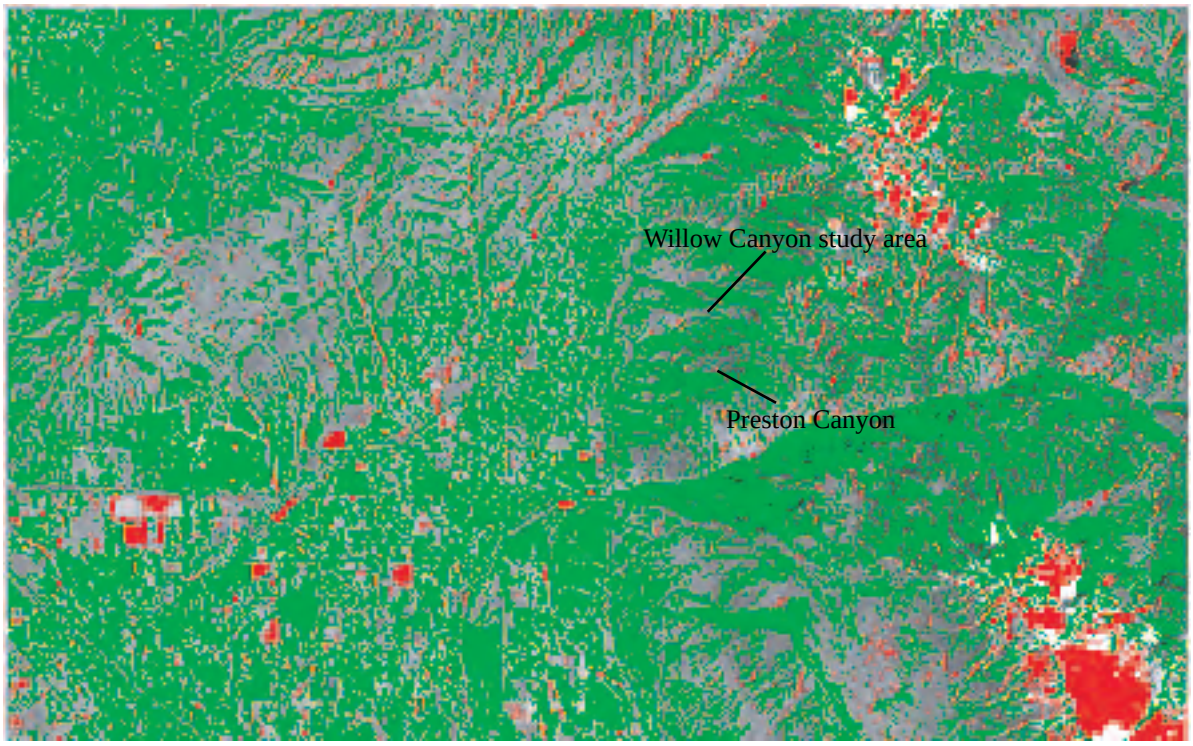

Figure 44: Alpine subset of Landsat 7 scene (band 8) overlain by +/- 10% change in band 5 between October 17. 1999 and May 28, 2000. Red shows areas of greater than 10% decrease and green shows areas of greater than 10% increase in brightness value.

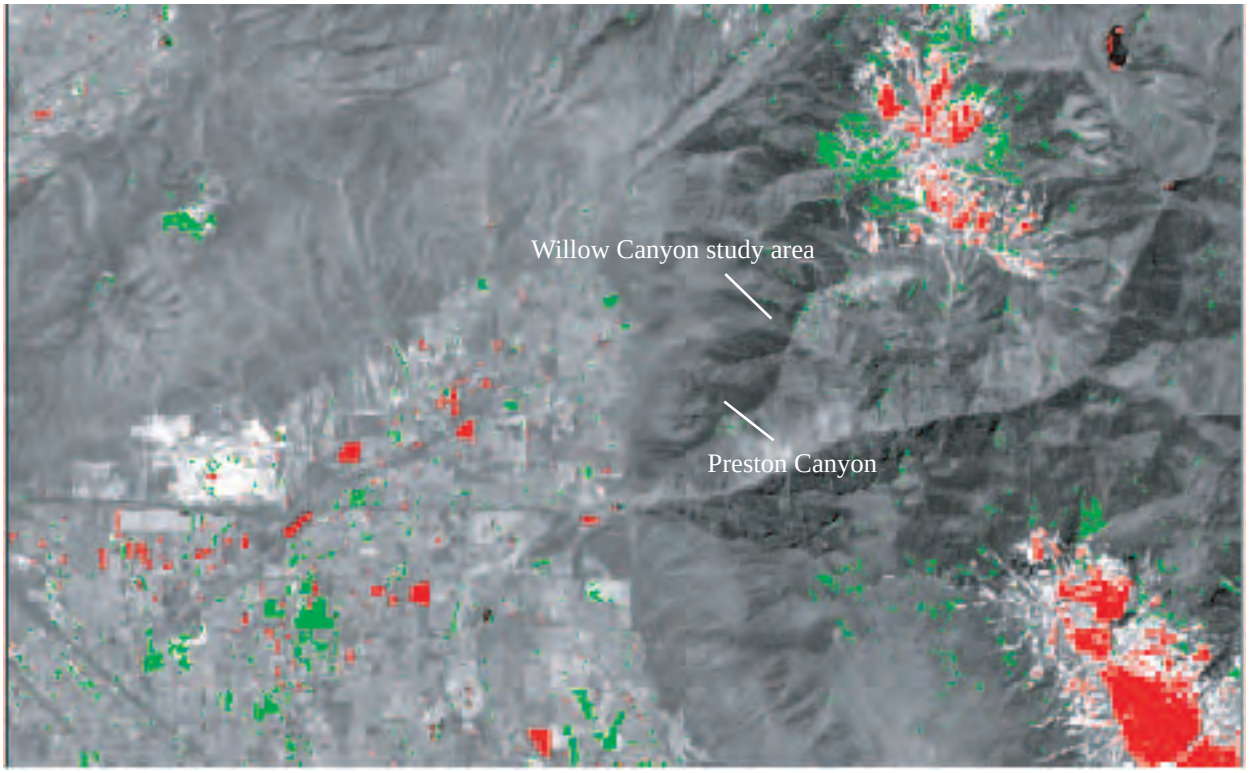

Figure 45: Alpine subset of Landsat 7 scene (band 8) overlain by +/- 30% change in band 5 between October 17. 1999 and May 28, 2000. Red shows areas of greater than 30% decrease and green shows areas of greater than 30% increase in brightness value.

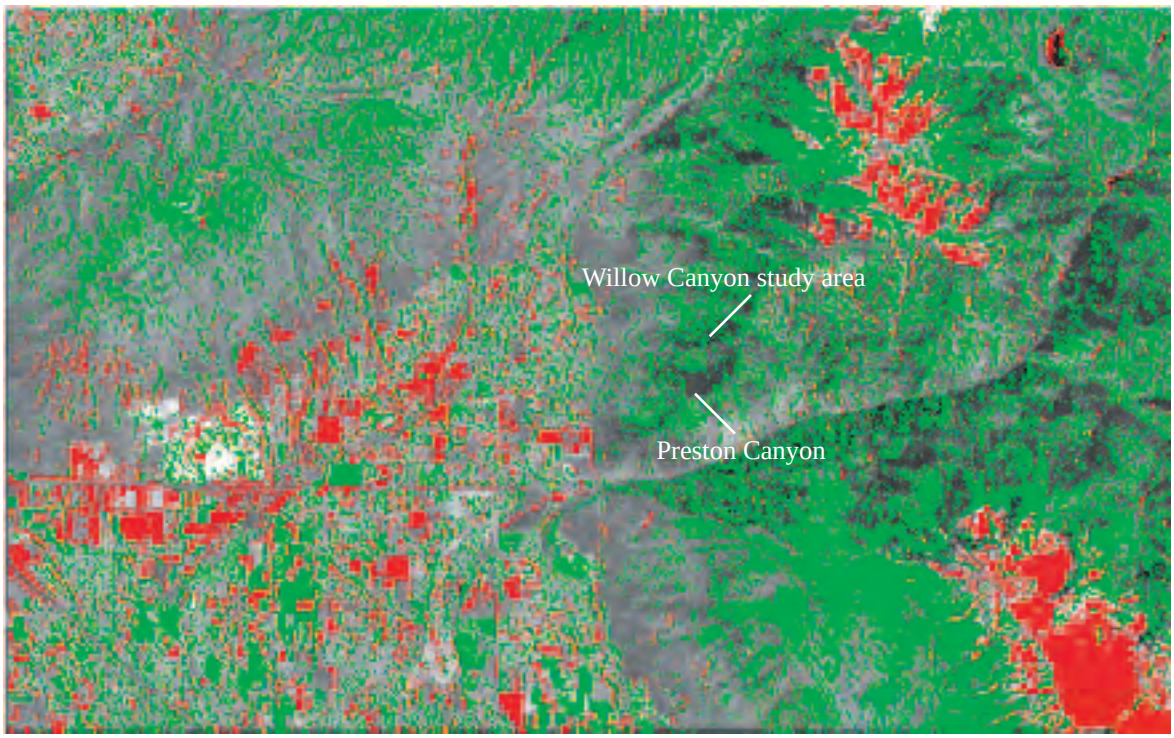

Figure 46: Alpine subset of Landsat-7 scene (bands 4, 3 and 2) overlain by +/- 10% change in band 5 between August 14. 1999 and May 28, 2000. Red shows areas of greater than 10% decrease and green shows areas of greater than 10% increase in brightness value.

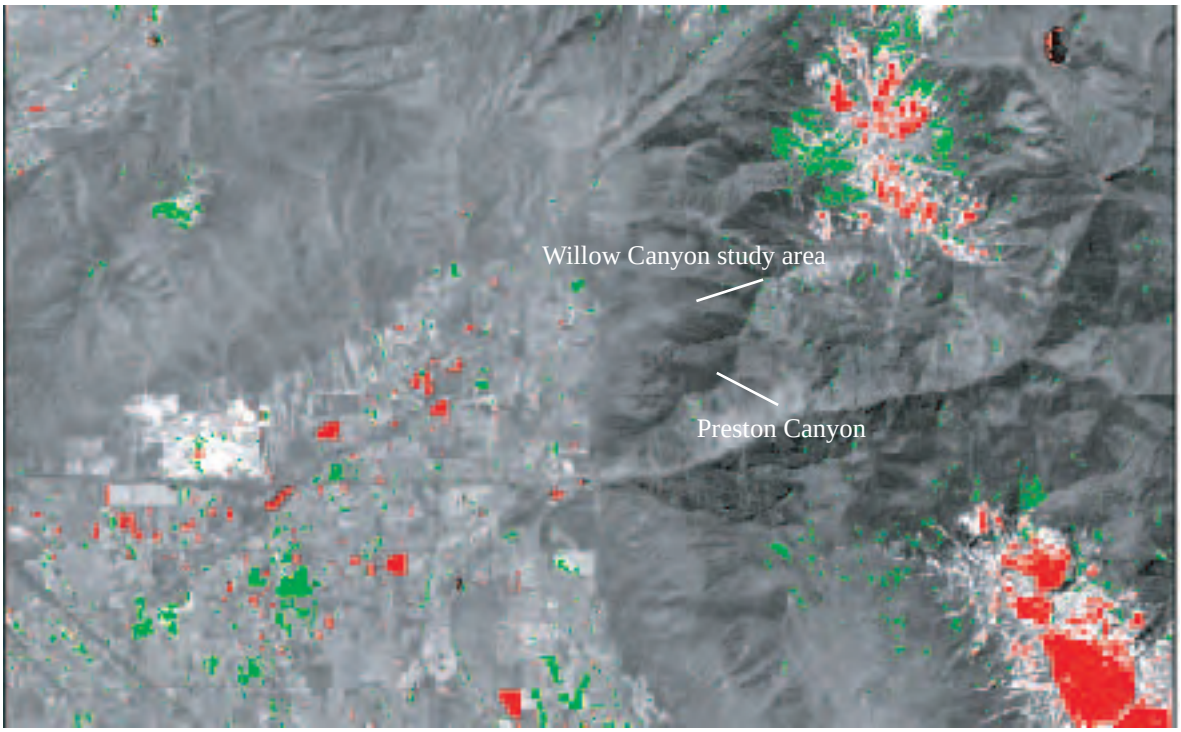

Figure 47: Alpine subset of Landsat-7 scene (bands 4, 3 and 2) overlain by +/- 30% change in band 5 between August 14. 1999 and May 28, 2000. Red shows areas of greater than 30% decrease and green shows areas of greater than 30% increase in brightness value.

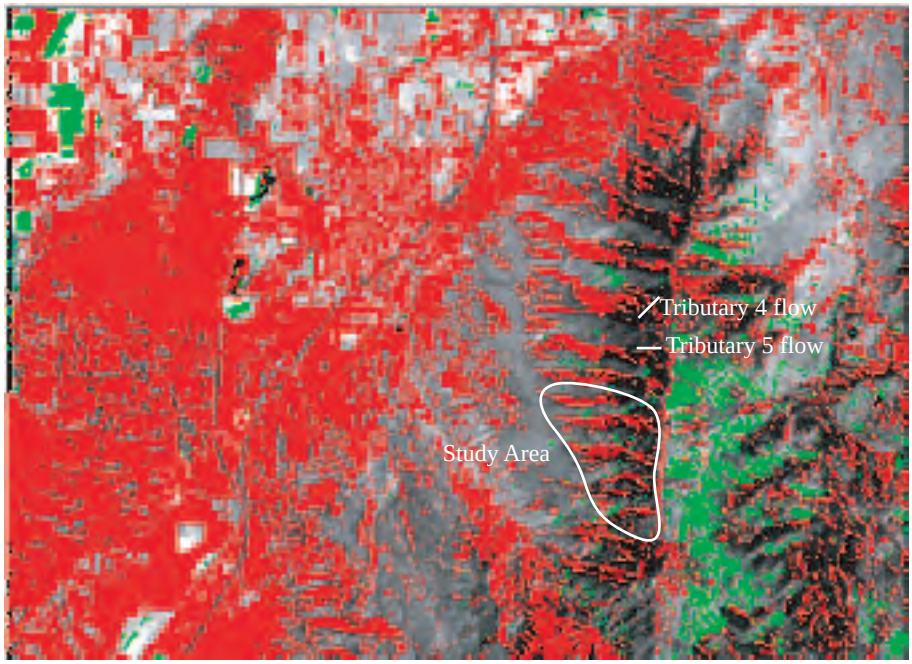

Figure 48: Santaquin subset of Landsat 7 scene (band 8) overlain by +/- 10% change in band 5 between August 14. 1999 and October 17, 1999. Red shows areas of greater than 10% decrease and green shows areas of greater than 10% increase in brightness value.

Figure 49: Santaquin subset of Landsat 7 scene (band 8) overlain by +/- 30% change in band 5 between August 14. 1999 and October 17, 1999. Red shows areas of greater than 30% decrease and green shows areas of greater than 30% increase in brightness value.

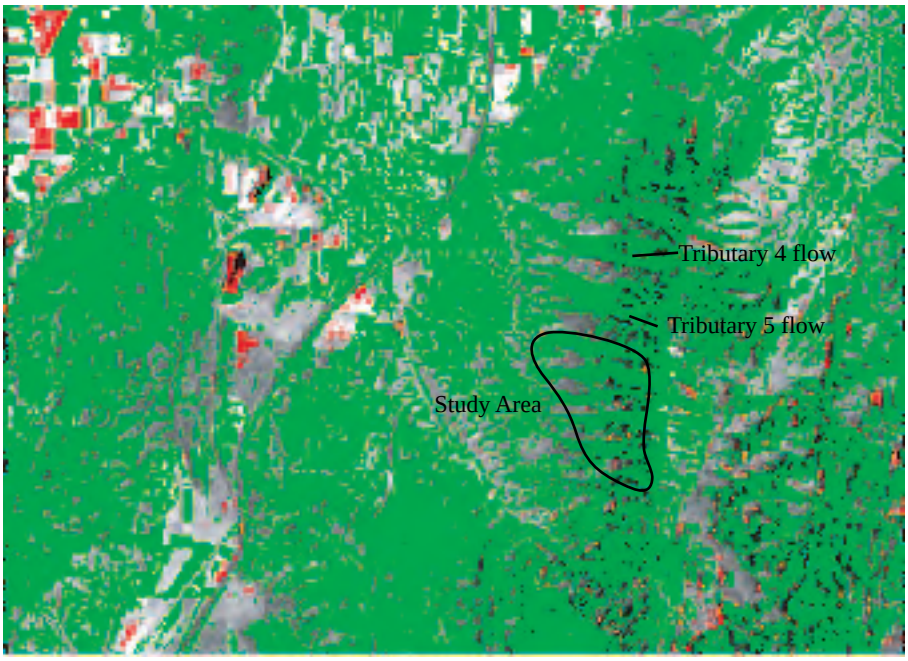

Figure 50: Santaquin subset of Landsat 7 scene (band 8) overlain by +/- 10% change in band 5 between October 17, 1999 and May 28, 2000. Red shows areas of greater than 10% decrease and green shows areas of greater than 10% increase in brightness value.

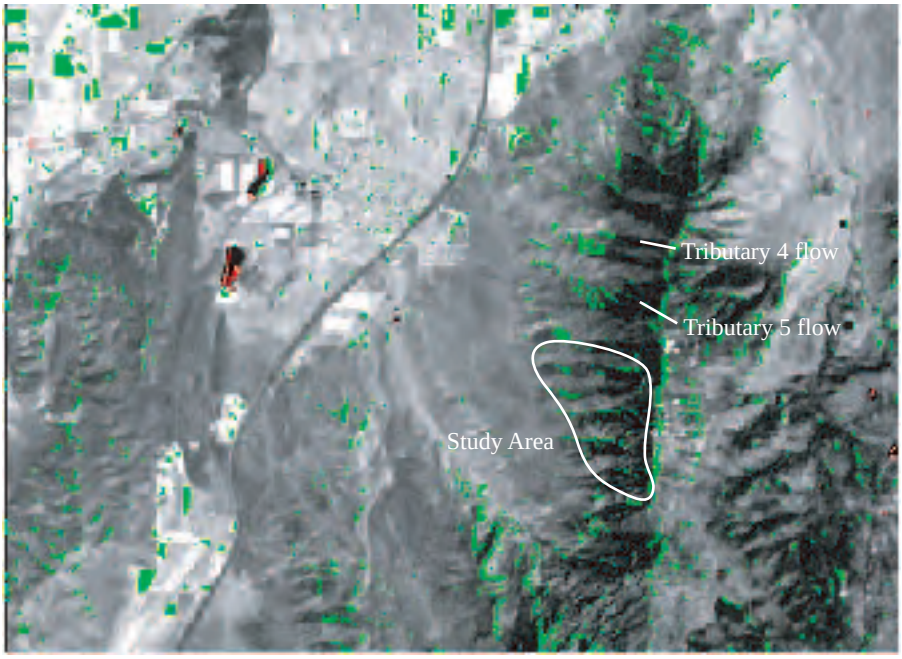

Figure 51: Santaquin subset of Landsat 7 scene (band 8) overlain by +/- 30% change in band 5 between October 17, 1999 and May 28, 2000. Red shows areas of greater than 30% decrease and green shows areas of greater than 30% increase in brightness value.

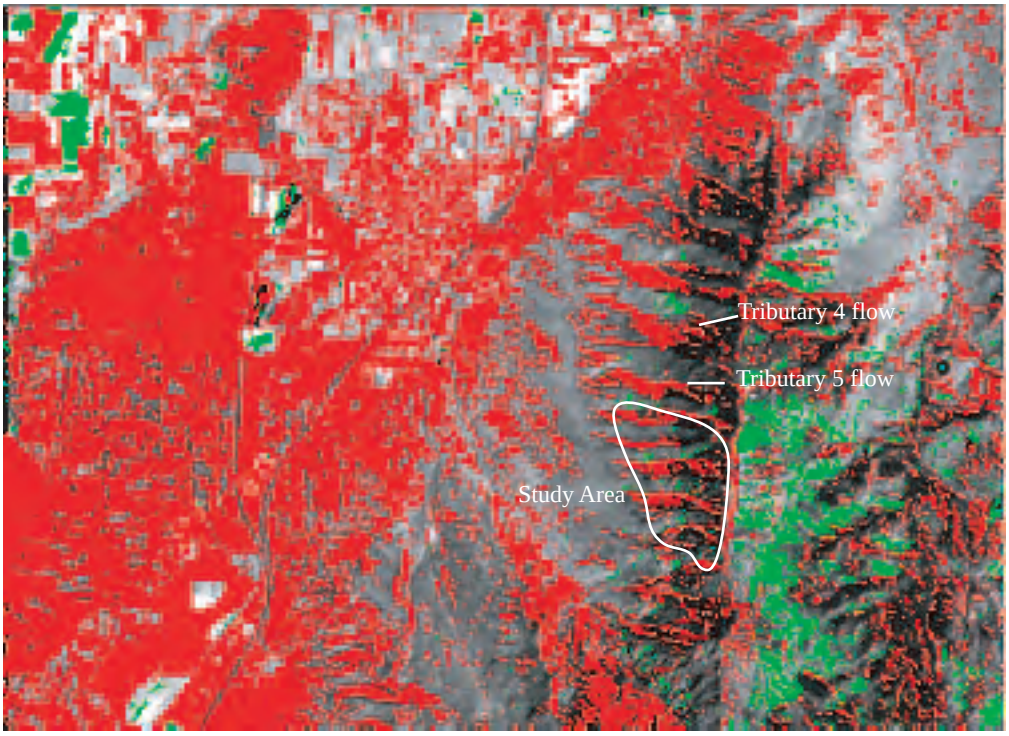

Figure 52: Santaquin subset of Landsat 7 scene (band 8) overlain by +/- 10% change in band 5 between August 14, 1999 and May 28, 2000. Red shows areas of greater than 10% decrease and green shows areas of greater than 10% increase in brightness value.

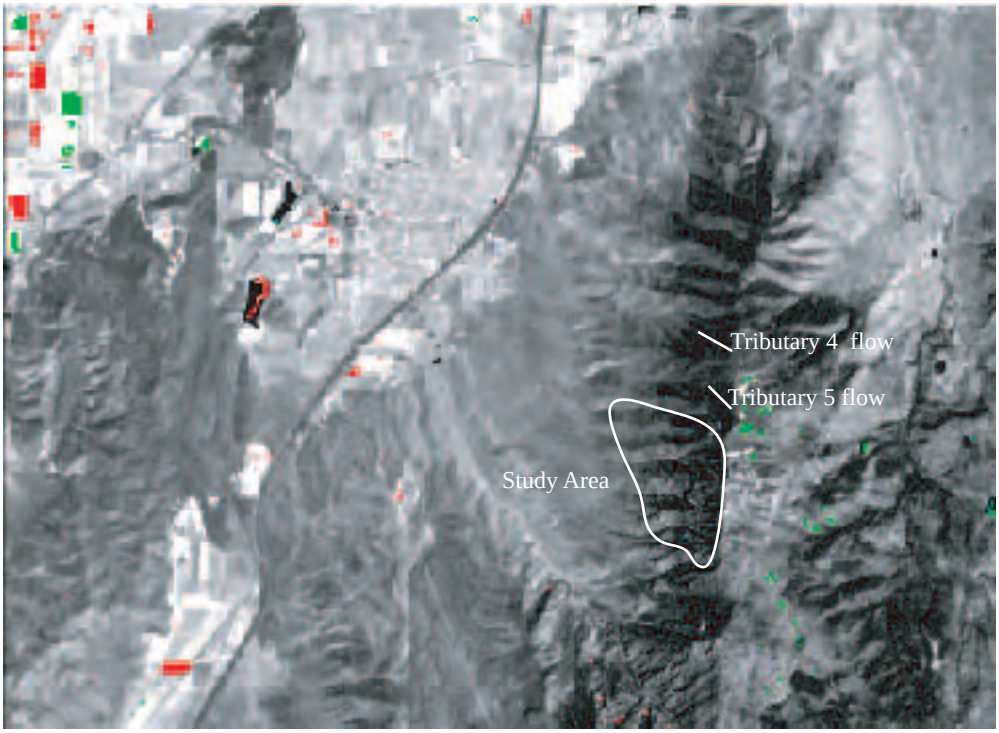

Figure 53: Santaquin subset of Landsat 7 scene (band 8) overlain by +/- 30% change in band 5 between August 14, 1999 and May 28, 2000. Red shows areas of greater than 30% decrease and green shows areas of greater than 30% increase in brightness value.

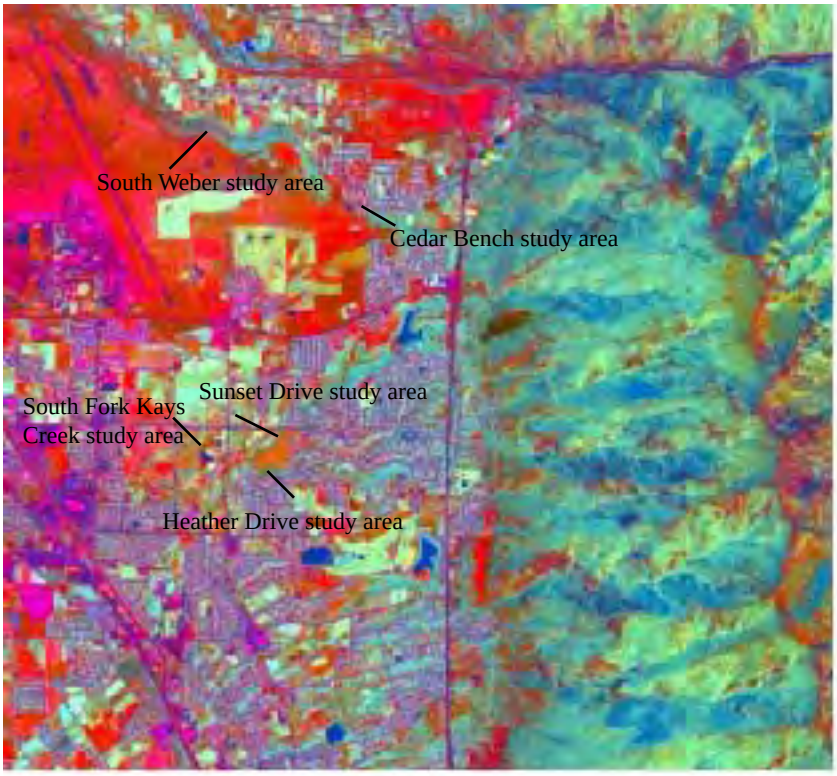

Figure 55: Layton subset (August 14, 1999) transformed using the tasseled cap transformation. Red or pink areas are high in brightness, green areas are high in greenness and blue areas are high in wetness or shadow.

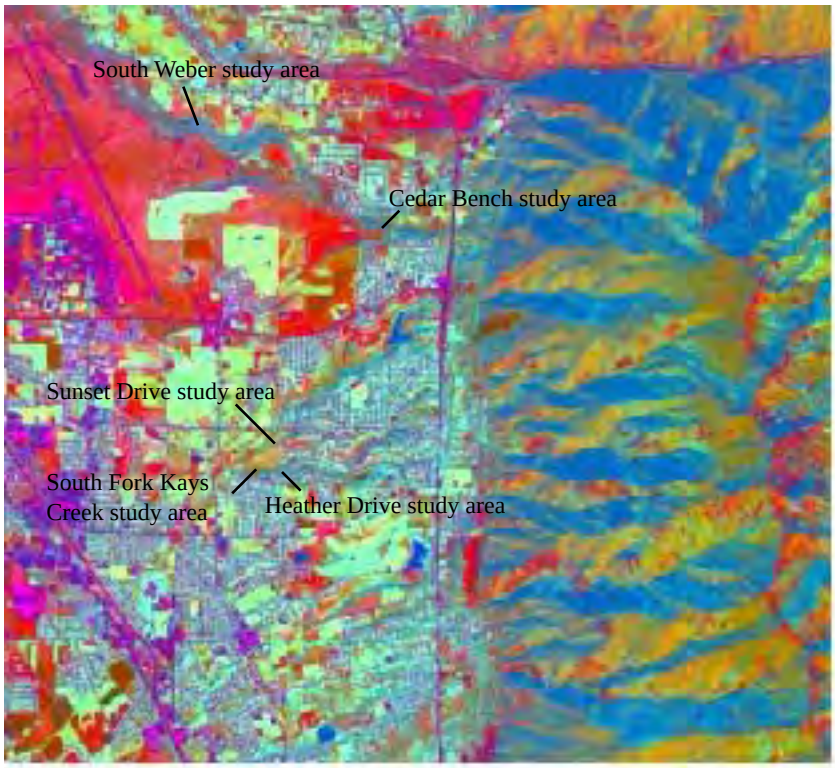

Figure 56: Layton subset (October 17, 1999) transformed using the tasseled cap transformation. Red or pink areas are high in brightness, green areas are high in greenness and blue areas are high in wetness or shadow.Note the strong decrease in greenness.

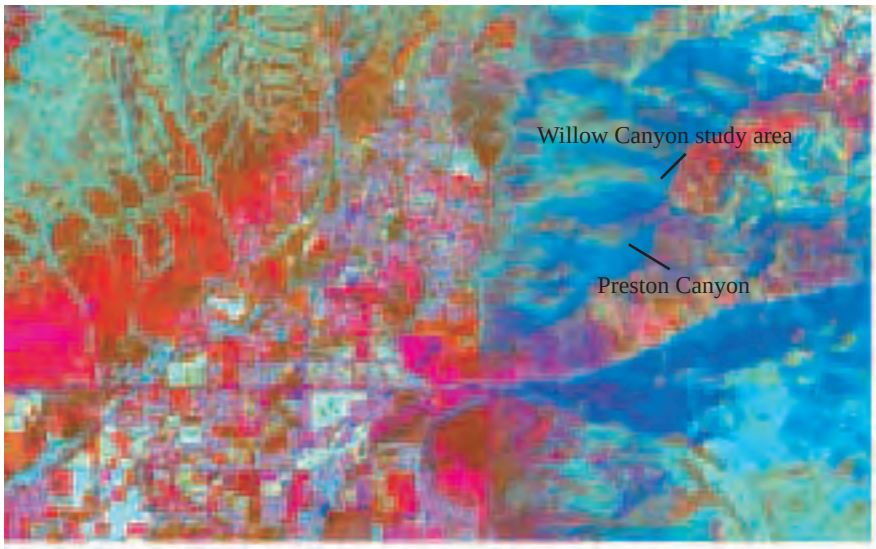

Figure 57: Alpine subset (August 14, 1999) transformed using the tasseled cap transformation. Red or pink areas are high in brightness, green areas are high in greenness and blue areas are high in wetness or shadow.

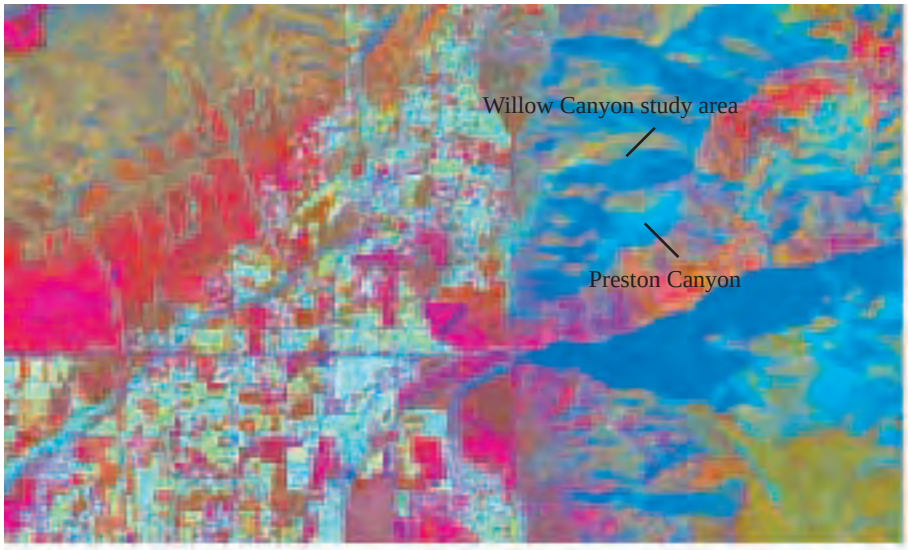

Figure 58: Alpine subset (October 17, 1999) transformed using the tasseled cap transformation. Red or pink areas are high in brightness, green areas are high in greenness and blue areas are high in wetness or shadow.As expected, there is a strong decrease in greenness.

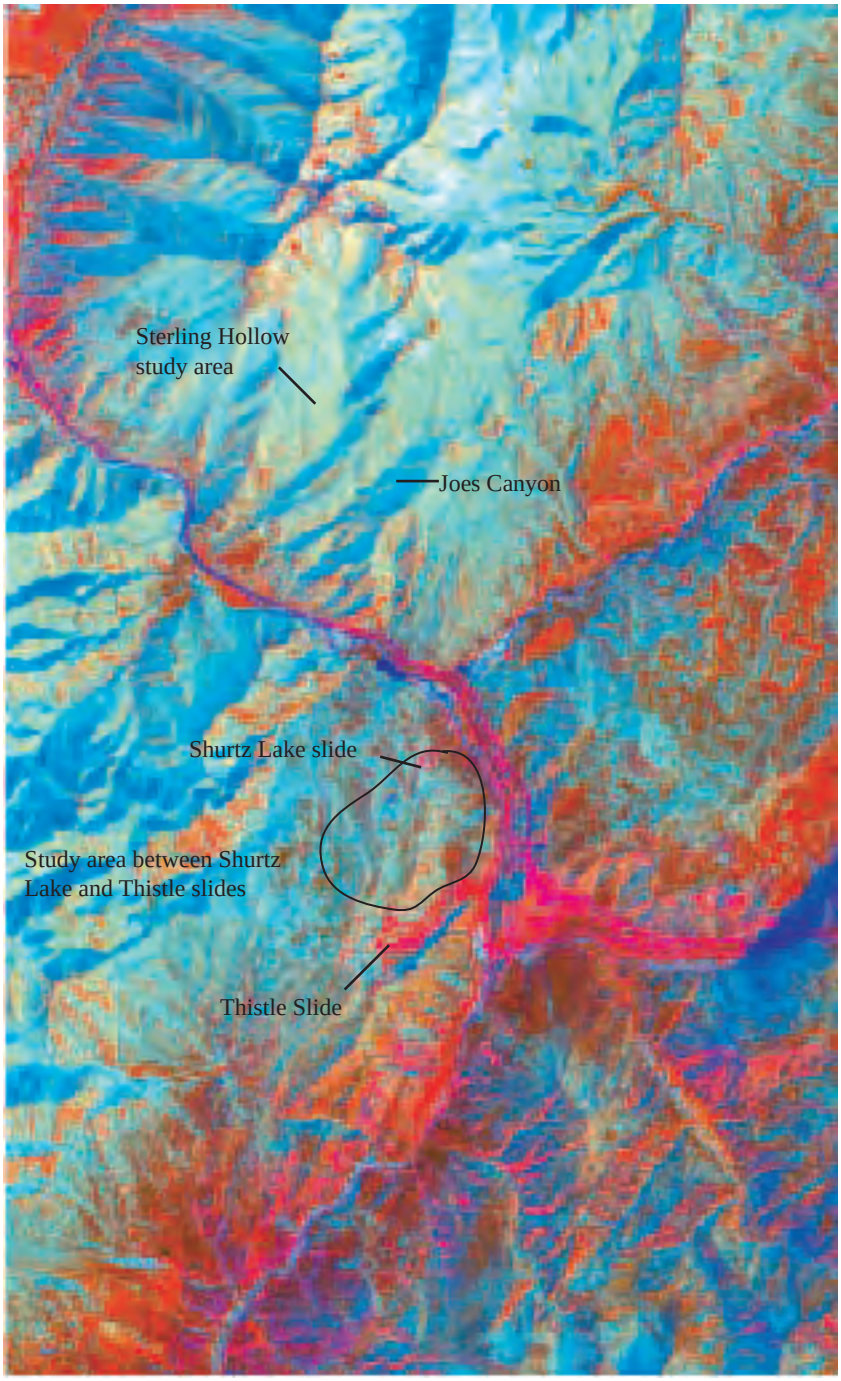

Figure 59: Spanish Fork subset (August 14, 1999) transformed using the tasseled cap transformation. Red or pink areas are high in brightness, green areas are high in greenness and blue areas are high in wetness or shadow.

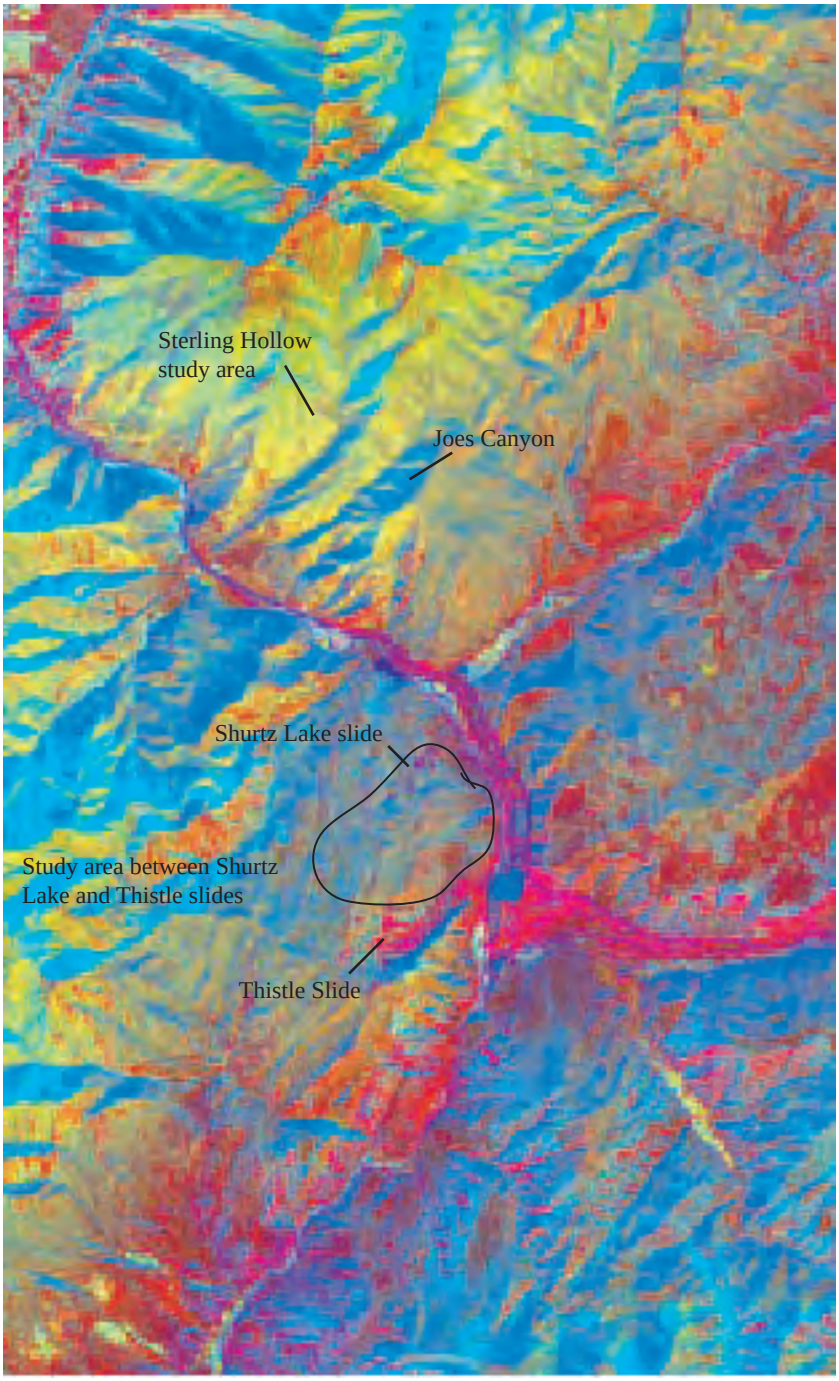

Figure 60: Spanish Fork subset (October 17, 1999) transformed using the Tasseled Cap transformation. Red or pink areas are high in brightness, green areas are high in greenness and blue areas are high in wetness or shadow.

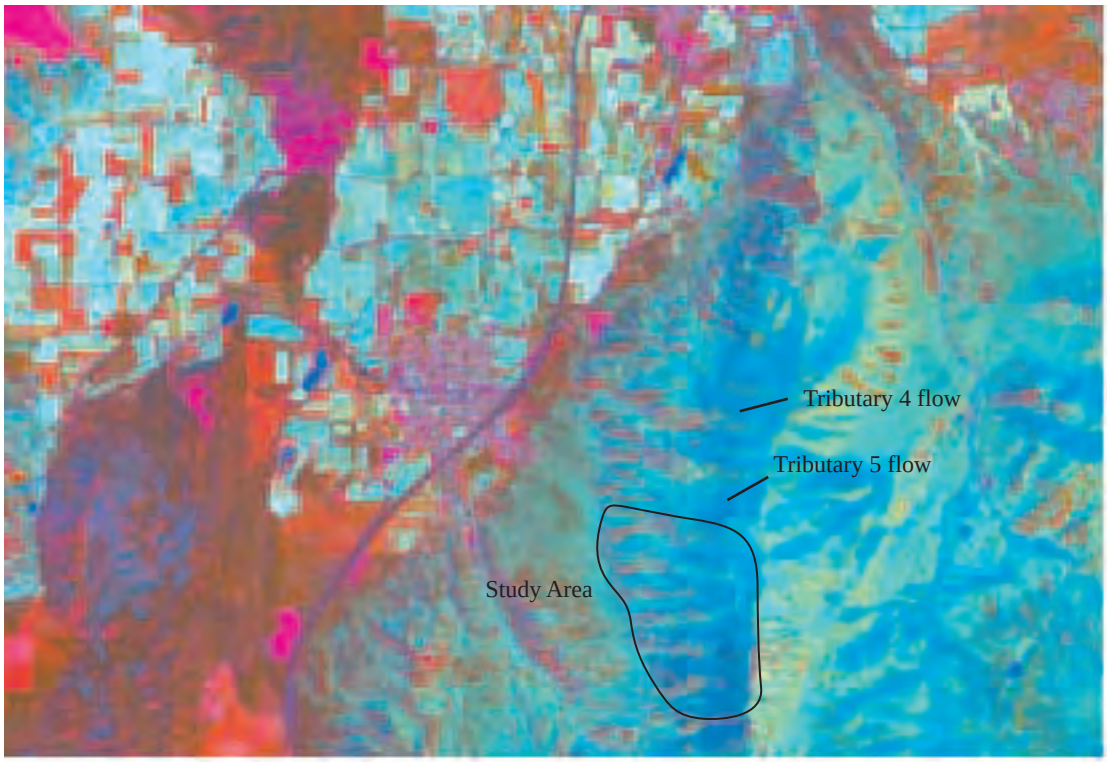

Figure 61: Santaquin subset (August 14, 1999) transformed using the tasseled cap transformation. Red or pink areas are high in brightness, green areas are high in greenness and blue areas are high in wetness or shadow.

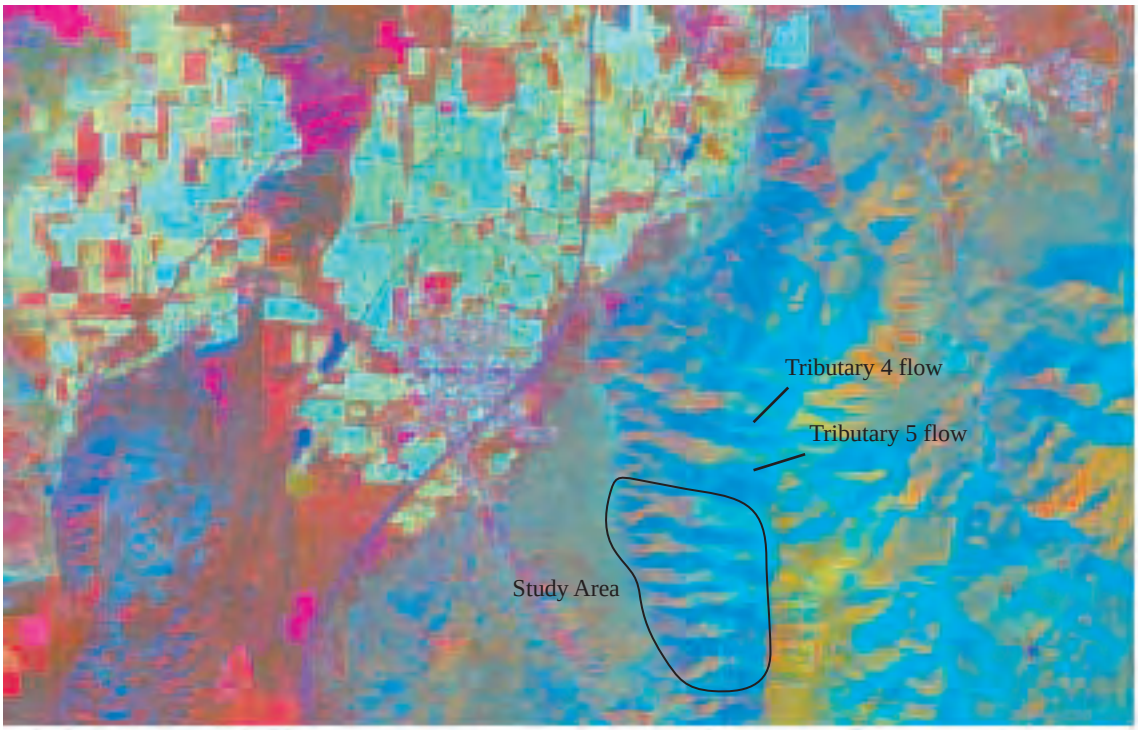

Figure 62: Santaquin subset (October 17, 1999) transformed using the tasseled cap transformation. Red or pink areas are high in brightness, green areas are high in greenness and blue areas are high in wetness or shadow.